Marine Geology 274 (2010) 135–150

Contents lists available at ScienceDirect

Marine Geology

journal homepage: www.elsevier.com/locate/margeo

Facies, $\delta^{13}C$, $\delta^{15}N$ and C/N analyses in a late Quaternary compound estuarine fill, northern Brazil and relation to sea level

Darciléa Ferreira Castro [a], Dilce de Fátima Rossetti [b,*], Luiz Carlos Ruiz Pessenda [c]

[a] Universidade de São Paulo-USP, Instituto de Geociências – Programa de Geotectônica e Geoquímica; Rua do Lago, 562 Cidade Universitária 05508-080 São Paulo, SP, Brazil
[b] Instituto Nacional de Pesquisas Espaciais-INPE, Rua dos Astronautas 1758-CP 515, 12245-970 São José dos Campos-SP, Brazil
[c] Universidade de São Paulo, Laboratório de ^{14}C, Av. Centenário 303, 13416000 Piracicaba, SP, Brazil

ARTICLE INFO

Article history:
Received 29 June 2009
Received in revised form 17 March 2010
Accepted 29 March 2010
Available online 8 April 2010

Keywords:
estuarine setting
sedimentary facies
isotopes
late Quaternary
relative sea-level

ABSTRACT

The present work integrates sedimentary facies, ^{14}C dating, $\delta^{13}C$, $\delta^{15}N$, and C/N with geologic and geomorphologic data available from literature. The aim was to characterize the depositional settings of a late Quaternary estuary in northeastern Marajó Island and analyze its evolution within the context of relative sea level fluctuations. The data derive from four continuous cores along a proximal-to-distal transect of a paleoestuary, previously recognized using remote sensing information. Fifteen sediment samples recorded ages ranging from 42,580 ± 1430 to 3184 ± 37 ^{14}C yr B.P. Facies analysis indicated fine- to coarse-grained sands with parallel lamination or cross stratification, massive or laminated muds and heterolithic deposits. $\delta^{13}C$ (−28.1‰ to −19.7‰, mean = −23.0‰), $\delta^{15}N$ (+14.8‰ to +4.7‰, mean = +9.2‰) and C/N (14.5 to 1.5, mean = 7.9) indicate mostly marine and freshwater phytoplankton sources for the organic matter. The results confirm a large late Quaternary paleoestuary in northeastern Marajó Island. The distribution of $\delta^{13}C$, $\delta^{15}N$, and C/N, together with facies associations, led to identify depositional settings related to fluvial channel, floodplain, tidal channel/tidal flat, central basin, tidal delta, and tidal inlet/sand barrier. These deposits are consistent with a wave-dominated estuary. Variations in stratigraphy and geochemistry are controlled by changes in relative sea level, revealing a main transgression from an undetermined time around 42,000 ^{14}C yr B.P. and 29,340 (± 200) ^{14}C yr B.P., which is synchronous to the overall drop in sea level after the last interglacial. Following this period, and probably until 9110 ± 37 ^{14}C yr B.P., i.e., during a time interval encompassing two glacial episodes including the Last Glacial and the Younger Dryas, there was a pronounced drop in sea level, recorded by the development of a major erosional discontinuity due to valley re-incision. Sea level rose again until 5464 ± 40 ^{14}C yr B.P, just before the main worldwide mid-Holocene transgressive peak. Mid to late Holocene coastal progradation ended the Marajó paleoestuarine history, and promoted the establishment of continental conditions throughout the island. The divergence comparing the Marajó sea level behavior with the eustatic curve allows hypothesizing that post-rifting tectonics along the Brazilian Equatorial margin influenced the sedimentary evolution of the studied paleoestuary. Considering that sedimentary facies in estuarine settings are highly variable both laterally and vertically, the present integration of facies with isotope and elemental analyses was crucial to provide a more precise interpretation of the Late Pleistocene and Holocene Marajó paleoestuary, and analyze its sea level history within the eustatic and tectonic context.

1. Introduction

In the last interglacial phase (120–130 ka BP), known as Sangamon interglacial in North America, the Ipswichian interglacial in the United Kingdom and the Riss-Würm interglacial in the Alps), the global sea-level was around 4 to 6 m above the modern one (Shackleton, 1988). This period was followed by a progressive decay, until the maximum drop of more than 100 m during the Last Glacial Maximum. During the middle Holocene, sea level rose at a maximum of nearly 5 m above modern sea-level, before its stabilization at the present position (e.g., Crowley and North, 1991). The reproduction of this sea level history along the Brazilian coast is an ongoing issue. In general, the last interglacial transgressive phase has been recorded only along a few areas in Northeastern and Southeastern Brazil, where it is known as the Penultimate and Cananéia Transgression, respectively (Martin et al., 1982, 1986; Suguio et al., 1985; Tomazelli and Dillenburg, 2007). In addition, despite the higher volume of studies focusing the Holocene sea level changes, this is still an issue of great debate, with no consensus neither on the magnitude of fluctuations nor on the chronology of the transgressive–regressive events. For instance, while some authors (e.g., Suguio et al., 1985 and Martin et al., 2003) have suggested rises of up to 5 m above the modern sea level during the

* Corresponding author. Tel.: +55 12 39456451; fax: +55 12 39456488.
E-mail addresses: darcicastro@yahoo.com.br (D.F. Castro), rossetti@dsr.inpe.br (D.F. Rossetti), pessenda@cena.usp.br (L.C. Ruiz Pessenda).

0025-3227/$ – see front matter © 2010 Elsevier B.V. All rights reserved.
doi:10.1016/j.margeo.2010.03.011

late Holocene transgression, as recorded in other areas of the South American coast (Milne et al. 2005), others (e.g., Angulo and Lessa 1997, Lessa and Angulo 1998, Angulo et al., 2006) have proposed rises of less than 1 m in the same time length.

The latest Quaternary sea level history in Northern Brazil is even less studied than in other areas of this country. For the Late Pleistocene, there is only one study based on a core data from Marajó Island recording a rise in relative sea level between 39 and 35 ka BP (Miranda and Rossetti, 2009). These authors have also reported another rise at the Late Pleistocene to Holocene transition, which lasted until the mid-Holocene, when the relative sea level progressively dropped (Miranda and Rossetti, 2009). A few other studies have reported a rise similar to the modern one during the early to mid Holocene (Behling and Costa, 2000, 2001; Behling, 2001; Behling et al., 2001a,b; Souza-Filho and Paradella, 2003; Cohen et al., 2004, 2005a,b; Vedel et al., 2006), with a mid-Holocene drop, followed by an overall transgression. Most of these studies are based on palynological data, and no emphasis has been placed on facies analysis aiming to determine the depositional environments in order to help reconstructing sea level fluctuations in Northern Brazil.

Research combining remote sensing and core data (e.g., Rossetti and Valeriano, 2007; Rossetti et al., 2007; Rossetti et al., 2008a) has shown that Quaternary deposits are well represented in Marajó Island, located at the Amazonas River mouth. A recent study (Rossetti et al., 2008b) based on Landsat images integrated with facies analysis has recorded a large Quaternary estuarine morphology in eastern Marajó, the origin and abandonment of which is related to tectonics. This provides an opportunity to analyze changes in relative sea level in Northern Brazil, as estuarine deposits form within incised valleys, where the sea level history might be better preserved, particularly in areas with low accommodation space.

The characterization of estuarine lithosomes is a complex task, because estuaries are sites of high lateral and vertical facies variability. The difficulty increases when interpretation relies only on core data, which preclude an adequate approach of spatial facies relationships. In this instance, combination of facies analysis with other paleoenvironmental proxies is highly desirable. $\delta^{13}C$, $\delta^{15}N$, and C/N analyses of organic matter preserved in sediments have been increasingly used to characterize both modern and ancient depositional environments (Shultz and Calder, 1976; Salomons and Mook, 1981; Sherr, 1982; Martinelli et al., 1988; Malamud-Roam and Ingram, 2004; Megens et al., 2002; Pessenda et al., 2004). $\delta^{13}C$ composition helps to distinguish between C_3 ($\delta^{13}C = -32.0‰$ to $-20.0‰$) and C_4 ($\delta^{13}C = -17.0‰$ to $-9.0‰$) photosynthetic plants (Deines, 1980; O'Leary, 1988; Lajtha and Marshall, 1994). These values show some overlapping with $\delta^{13}C$ from marine organic matters, which range from $-25.0‰$ to $-20.0‰$ (Fry and Sherr, 1984; Middelburg and Nieuwenhuize, 1998; Wilson et al., 2005a). For this reason, $\delta^{13}C$ has been combined with $\delta^{15}N$ and C/N for distinguishing sources of organic matter in sedimentary deposits derived from many recent and ancient estuarine environments (Meyers, 1994, 1997; Thornton and McManus, 1994; Cloern et al., 2002; Graham et al., 2001; Ogrinc et al., 2005; Wilson et al., 2005b). According to these authors, $\delta^{15}N$ allows distinction between organic matter derived from land vascular plants (values around 0.0‰) and phytoplankton (values around 10.0‰).

In addition to $\delta^{13}C$ and $\delta^{15}N$, the C/N values obtained from total organic carbon (TOC) and total nitrogen (TN), help to discriminate between freshwater/marine phytoplankton ($C/N = 4.0$ to 10.0) and land vascular plant ($C/N \geq 12.0$) (e.g., Cloern et al., 2002; Meyers, 2003; Wilson et al., 2005a). Integrated with facies analysis, these proxies have the potential to provide a more precise reconstruction of depositional environments within estuarine systems, particularly when only core data are available.

Several authors have discussed the effect of diagenesis on $\delta^{13}C$, $\delta^{15}N$ and C/N signals of organic matter preserved in sediments (see Chen et al., 2008 for a review). In general, the authors agree on a rapid biodegradation of the organic matter still in the water column, which might be reflected in the primary isotopic values. Although not of a common sense yet (e.g., see discussion in Lamb et al., 2006 and Chen et al., 2008), many authors (e.g., Thornton and McManus, 1994; Middelburg and Nieuwenhuize, 1998; Cloern et al., 2002) have proposed that, once buried, the organic matter preserved on sediments will display minor changes in $\delta^{13}C$ and total carbon (TC) and total nitrogen (TN), which allow their use as reliable geochemical proxy indicators. In contrast, the $\delta^{15}N$ signal of buried organic matter is more variable due to biodegradation, and mostly contamination, by inorganic nitrogen. Although this fact might reduce its potential for paleoenvironmental reconstructions, $\delta^{15}N$ might add information to $\delta^{13}C$ and C/N, helping with interpretation.

The main goal of this work is to characterize the depositional environments in the late Quaternary estuarine system in eastern Marajó Island through integration of facies analysis, ^{14}C dating, $\delta^{13}C$, $\delta^{15}N$ and C/N. The investigation provided faciological parameters that help to define the estuary type and to discuss its evolution through time within the context of late Quaternary relative sea level fluctuations, providing comparisons with the late Quaternary global sea-level changes. Furthermore, confirmation of this palaeoestuary, previously suggested using remote sensing techniques, offers a valuable opportunity to evaluate the results of integrating facies analysis with $\delta^{13}C$, $\delta^{15}N$ and C/N as proxy indicators for characterizing ancient estuarine settings in core data.

2. Geologic framework

Eastern Marajó Island is located in a poorly-known geological setting referred as the Pará Platform, a structure bounded by the Mexiana Sub-Basin to the northwest, Limoeiro Sub-Basin of the Marajó Graben System to the southwest, and Pará–Maranhão Basin to the southeast (Fig. 1A). Rather than a tectonically stable area among sedimentary basins, this platform displays small, but deep, tectonic troughs, one of them been located in the deep sub-surface of the study area. This depression, recorded by a Bouguer anomaly, has a north–south orientation, extending northward, where it connects to the Mexiana Sub-Basin. The origin of this sub-basin is linked to the establishment of the Marajó Graben System through crustal stretching due to the opening of the South Atlantic Ocean, initiated in the Jurassic–Cretaceous boundary.

Based on sub-surface information, the sedimentary fill of the Mexiana Basin includes sandy and conglomeratic deposits of the Breves and Jacarezinho Formations (Aptian–Cenomanian), silty mudstones of the Anajás Formation (early Cretaceous), and sandstones, mudstones and conglomerates of the Limoeiro Formation (late Cretaceous). These units (Fig. 1B), formed in depositional settings ranging from alluvial fan, fluvial to shallow marine, are overlain by the Marajó (Paleocene–Eocene) and the Tucunaré/Pirarucu (Quaternary) Formations. The first consists of mixed siliciclastic-limestones, while the latter include sandstones and mudstones formed in shallow marine to fluvial–transitional settings, respectively.

At the surface, eastern Marajó Island displays a belt of mostly estuarine sandstones and mudstones of the Barreiras Formation (Rossetti, 2000). This unit (Fig. 1B) is unconformably overlain by eolian and fluvio-estuarine sands and muds inserted in the lithostratigraphic term of Post-Barreiras Sediments (Plio-Pleistocene to Holocene), which includes the deposits characterized herein. The Post-Barreiras Sediments are a result of normal and strike-slip faults (Costa et al., 2001, 2002).

Fault reactivation during the Late Pleistocene and Holocene would have led to the establishment of the estuarine system under investigation, followed by its abondonment, (Rossetti et al., 2007; Fig. 1A). This paleomorphology, located circa 40 km south from the modern coastline, is up to 25 km wide and 50 km long. It displays a funnel shape, with the wide edge opening to the north and the

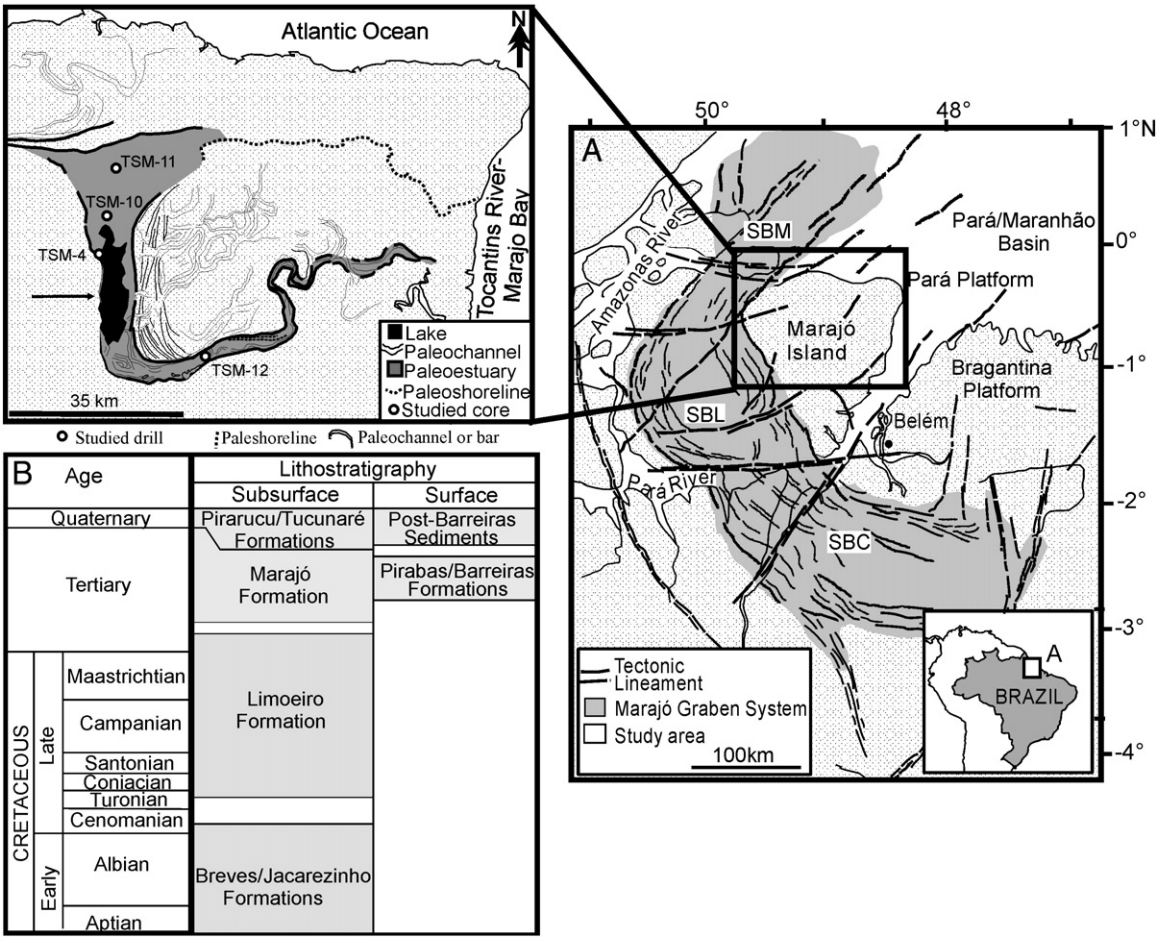

Fig. 1. A) Location map of the study area in eastern Marajó Island, northern Brazil (SBM = Mexiana Sub-Basin; SBL = Limoeiro Sub-Basin; SBC = Cametá Sub-Basin). B) Chart summarizing the stratigraphy of the study area.

narrower edge to the south and east, where the estuary grades into elongated meandering channels.

3. Material and methods

Marajó Island is part of a fluvio-marine archipelago bounded by the Atlantic Ocean to the north, the Pará River to the south, the Tocantins River-Marajó Bay to the east, and the lower Amazon River to the west (Fig. 1A). The climate is tropical, with a mean annual temperature of 28 °C and precipitation of 2500 to 3000 mm/yr. The topography is low, being represented by a mean altitude of 12.5 m for the entire island, and between 2 and 6 m for the eastern side of the island, where the study area is located.

The methods included analyses of sedimentary facies, $\delta^{13}C$, $\delta^{15}N$, C/N within a radiocarbon dating framework. The cores were obtained using a percussion drilling Robotic Key System (RKS), model COBRA mk1 (COBRA Directional Drilling Ltd., Darlington, U.K.). Four continuous cores, each up to 24 m in thickness, were retrieved from four drilling sites (TSM4, TSM10, TSM11 and TSM12). Based on the established palaeoestuarine morphology (Rossetti et al., 2007), the core sites were orientated along a proximal (south to northeast)–distal (north) transect (see blow out in Fig. 1A for core location within the paleoestuary). Features such as lithology, sedimentary structure, stratigraphic surface and fossil content, were recorded on all cores using vertical lithostratigraphic profiles.

For the TOC, TN and isotope analyses, a total of 76 core samples were oven dried at 50 °C and homogeneized. A parcel (around 1 g) from each sample was acidified with 1.5 N HCl to remove inorganic carbon. The analyses were performed at the Stable Isotope Laboratory of Center for Nuclear Energy in Agriculture (CENA). The TOC and TN were measured from a same parcel, and provided data for determining the C/N values. Isotopic and geochemical analyses were conducted on an elementary analyzer attached to a Mass Spectrometry ANCA SL 2020 of Scientific Europa. The $\delta^{13}C$ and $\delta^{15}N$ values are presented in ‰ relative to the PDB (Pee Dee Belemite) standard and atmospheric N_2, respectively. Results are expressed in percentage of dry weight (total C and N) and as $\delta^{13}C$ and $\delta^{15}N$ with respect to the VPDB (Viena Pee Dee Belemnite) standard and atmospheric N_2, respectively, using the conventional δ (‰) notations. Analytical precision is $\pm 0.1\%$ and $\pm 0.2‰$ for the C and N, respectively.

Fourteen wood, charcoal and organic sediments were dated by accelerator mass spectrometer (AMS) at the Beta Analytic Radiocarbon Dating Laboratory. Possible contaminants, as modern roots, were eliminated mechanically during the pre-treatment. In the following, the organic matter from sediments was extracted according to the laboratory standard pre-treatment with acid–alkali–acid wash. This procedure attempted to remove recent organic matter or ancient organic matter in process of slow decomposition that are adsorbed in the sediments, and which could provide carbon that are younger than the average carbon in the samples. The serial rinses eliminated all mechanical contaminants as associated sediments and rootlets. Conventional ^{14}C ages were calibrated to calendar years using the Pretoria Calibration Procedure program (Talma and Vogel, 1993).

4. Age and stratigraphy

The ^{14}C ages for the studied deposits are shown in Table 1, and the stratigraphic positions of the analyzed samples are plotted along the

Table 1
Radiocarbon ages obtained for the Quaternary deposits studied in eastern Marajó Island. All ages were analyzed by AMS.

Core	Sample	Depth (m)	^{14}C yr B.P.	Cal year B.P. 2-sigma calibration
TSM4	MR232	2.3	4,940 (±40)	5,740–5,600
	MR237	4.9	7,510 (±50)	8,400–8,200
	MR241	7.9	7,450 (±40)	8,360–8,180
	MR 248	11.8	41,582 (±1432)	–
	MR 249	12.5	42,580 (±1430)	–
TSM10	MR 352	17.9	6,010 (±40)	6,950–6,740
	MR355	19.1	6,360 (±50)	7,420–7,170
	MR365	23.0	29,340 (±200)	–
TSM11	MR369	3.0	3,184 (±37)	3,436–3,241
	MR372	5.3	5,330 (±40)	6,210–5,990
	MR381	9.8	5,464 (±40)	4,349–4,225
	MR385	11.6	5,590 (±40)	6,440–6,300
	MR392	15.0	8,473 (±39)	7,579–7,448
	MR397	17.9	9,110 (±37)	8,320–8,222
TSM12	MR408	6.8	5,800 (±50)	6,730–6,480

profiles of Figs. 2–5. The results were consistent, indicating a progressive age increase with depth. Maximum and minimum ages are 42,580 (±1430) and 3184 (±37) ^{14}C yr B.P., respectively, suggesting that the sediments were deposited mostly during the Late Pleistocene and Holocene.

The oldest ages (41,582±1432 and 42,580±1430 ^{14}C yr B.P.) are recorded below only 12 m depth in drill TSM4, directly underlying a discontinuity surface. The next oldest age of 29,340 (±200) ^{14}C yr B.P. was also recorded underlying a discontinuity surface, corresponding to a sample collected below 23 m depth in drill TSM10. The discontinuity surface in this drill is mantled by limestone pebbles. The remaining samples recorded only Holocene ages ranging from 9110±37 to 3184±37 ^{14}C yr B.P. Taking the radiocarbon ages into account, the stratigraphic correlation shows significant vertical displacements (Fig. 6).

5. Facies description

The deposits consist mostly of fine- to coarse-grained sands with parallel lamination or cross stratification, massive or laminated muds, and heterolithic deposits (Fig. 7A–G). These lithologies are arranged into coarsening and fining upward successions. Facies characteristics were added to δ^{13}C, δ^{15}N and C/N values in order to define six facies associations, which are representative of depositional environments typical o estuarine settings (Table 2, Figs. 2–5).

5.1. Facies association A (fluvial channel)

This association was recognized only in TSM4 and TSM12, between 11.0–13.7 m and 8.2–11.2 m, respectively (Figs. 2 and 5). These deposits consist mainly of fine to medium-grained sands that are either cross-stratified (facies Sc) or massive (facies Mm) and display bases defined by sharp and erosive surfaces that bound fining upward successions. These basal surfaces are locally mantled by pebbles of mudstone, sandstone or ferruginous concretions up to 2 cm in length. Facies association A is thin (i.e., a few centimeters thick) in TSM4, but it reaches up to 2.2 m in TSM12. Carbonized plant debris are found in association A. The isotope and elemental analyses of samples derived from this facies association indicated δ^{13}C = −27.8 to 24.8‰ (mean = −25.8‰), δ^{15}N = +7.1 to +12.7‰ (mean = +7.10‰), C/N = 8.0 to 13.0 (mean = 11).

5.2. Facies association B (floodplain)

This association occurs mainly in TSM4 and TSM12, corresponding to depth intervals of 11.0–13.7 m and 7.8–11.3, respectively (Figs. 2 and 5). These deposits consist typically of massive muds (facies Mm), which are interbedded with both lenticular/streaky (facies Hls) and wavy (facies Hw) heterolithic deposits. Facies association B is closely related to facies association A (fluvial channel). These tend to grade into each other forming fining upward cycles. The isotope and elemental analyses of samples derived from this facies association are similar to the previous association, indicated by δ^{13}C = −28.1 to −23.6‰ (mean = −26.‰); δ^{15}N = +5.8 to +11.8‰ (mean = +8.3‰); C/N = 5.2 to 14.5 (mean = 10.9).

5.3. Facies association C (tidal channel/tidal flat)

This facies association was described in all drills of the study area, occurring in the following depth intervals: 10.0–10.8 m and 13.70–16.2 m in TSM4; 19.8–24.0 m in TSM10 (Fig. 3); 9.2–9.9 m, 11.0–13.6 m and 15.0–18.0 m in TSM11 (Fig. 4); and 1.8–7.8 m in TSM12 (Fig. 5). These deposits either overly or underlie facies associations A and B in TSM4 and TSM12. Likewise association A, association C is represented mostly by fine to medium-grained, either cross-stratified (facies Sc) or massive (facies Sm) sands. Where cross beds are present, reactivation surfaces covered by mud drapes are frequent. Lenticular/streaky (facies Hls), wavy (facies Hw) and, locally, flaser (facies Hf) heterolithic deposits, as well as either massive (facies Mm) or laminated (facies Ml) muds and massive pelites (facies Pm) are present. These facies define fining upward successions averaging 1.0 m thick, which are bounded by sharp and erosive basal surfaces, locally overlain by mud intraclasts. Carbonized plant debris, as well as undetermined trace fossils, are present in this facies association. The isotope and elemental values differ from associations A and B. Hence, the carbon isotope values have a wider range, with an average toward heavier values, as indicated by δ^{13}C = −25 to −19.7‰ (mean = −22.6‰). On the other hand, the nitrogen values are, in general, comparable to those facies associations, ranging from δ^{15}N = +5.4 to +14.8‰, but with a slightly lower mean = +9.0‰. However, there is a significant change in the C/N ratio, which range from 3.4 to 10.2, with a mean of 5.1 (almost half of facies association A and B).

5.4. Facies association D (central basin)

Except for TSM12, this association was recorded in all the other drills. This facies unit is well represented in TSM10, between 0.4–8.3 m and 12.2–18.2 m (Figs. 3 and 4), and also present in TSM4 (Fig. 2), between 0.30–8.10 m and 8.1–10.8 m, being interbedded in the latter with facies association E (described below). Facies association D grades into facies association C in TSM11 (Fig. 4), between 8.4–9.1 m, 9.9–11 m and 13.6–15 m. This facies unit attains its greatest thickness in central and distal areas of the paleoestuary. Deposits in this association are essentially muddy, being represented by either massive (facies Mm) or parallel laminated (facies Ml) muds, massive pelites (Pm), as well as lenticular and streaky (facies Hls) and wavy (Hw) heterolithic deposits. Among these, facies Mp dominates, followed by facies Mm and Hls/Hw. Facies Pm occurs at the top of the mud succession, where it is locally associated with pedogenetic horizons. These paleosols consist of slightly endured, massive deposits with root marks, which grade downward into well structured deposits. Carbonized plant and coal fragments are disperse throughout this association. Facies association D display isotope and

Fig. 2. Lithostratigraphic profile from TSM 4, illustrating facies and facies associations, as well as position of the analyzed samples with their respective δ^{13}C, δ^{15}N, TOC (total organic carbon), TN (total nitrogen), and C/N values. Also included in this figure, as well as in Figs. 3–5, is the interpretation of marine (M) or continental (C) influence, based on an approximate estimation comparing the relative distribution of elemental and isotope values for each sample.

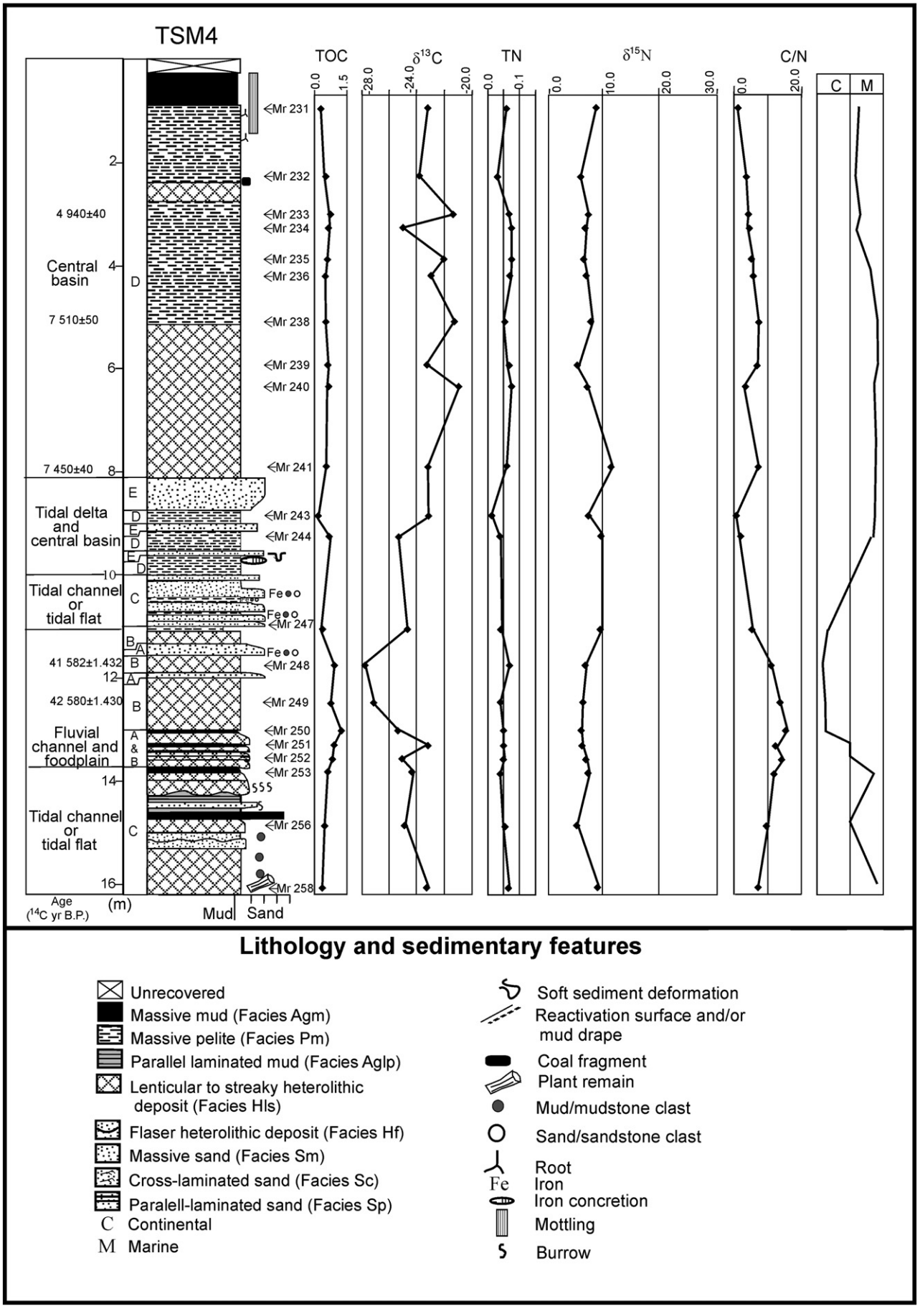
TSM4
TOC
δ13C
TN
δ15N
C/N
C
M
Mr 231
Mr 232
Mr 233
Mr 234
Mr 235
Mr 236
Mr 238
Mr 239
Mr 240
Mr 241
Mr 243
Mr 244
Mr 247
Mr 248
Mr 249
Mr 250
Mr 251
Mr 252
Mr 253
Mr 256
Mr 258
4 940±40
7 510±50
7 450±40
41 582±1.432
42 580±1.430
Central basin
Tidal delta and central basin
Tidal channel or tidal flat
Fluvial channel and foodplain
Tidal channel or tidal flat
Age (14C yr B.P.)
(m)
Mud
Sand
Lithology and sedimentary features
Unrecovered
Massive mud (Facies Agm)
Massive pelite (Facies Pm)
Parallel laminated mud (Facies Aglp)
Lenticular to streaky heterolithic deposit (Facies Hls)
Flaser heterolithic deposit (Facies Hf)
Massive sand (Facies Sm)
Cross-laminated sand (Facies Sc)
Paralell-laminated sand (Facies Sp)
C Continental
M Marine
Soft sediment deformation
Reactivation surface and/or mud drape
Coal fragment
Plant remain
Mud/mudstone clast
Sand/sandstone clast
Root
Fe Iron
Iron concretion
Mottling
Burrow

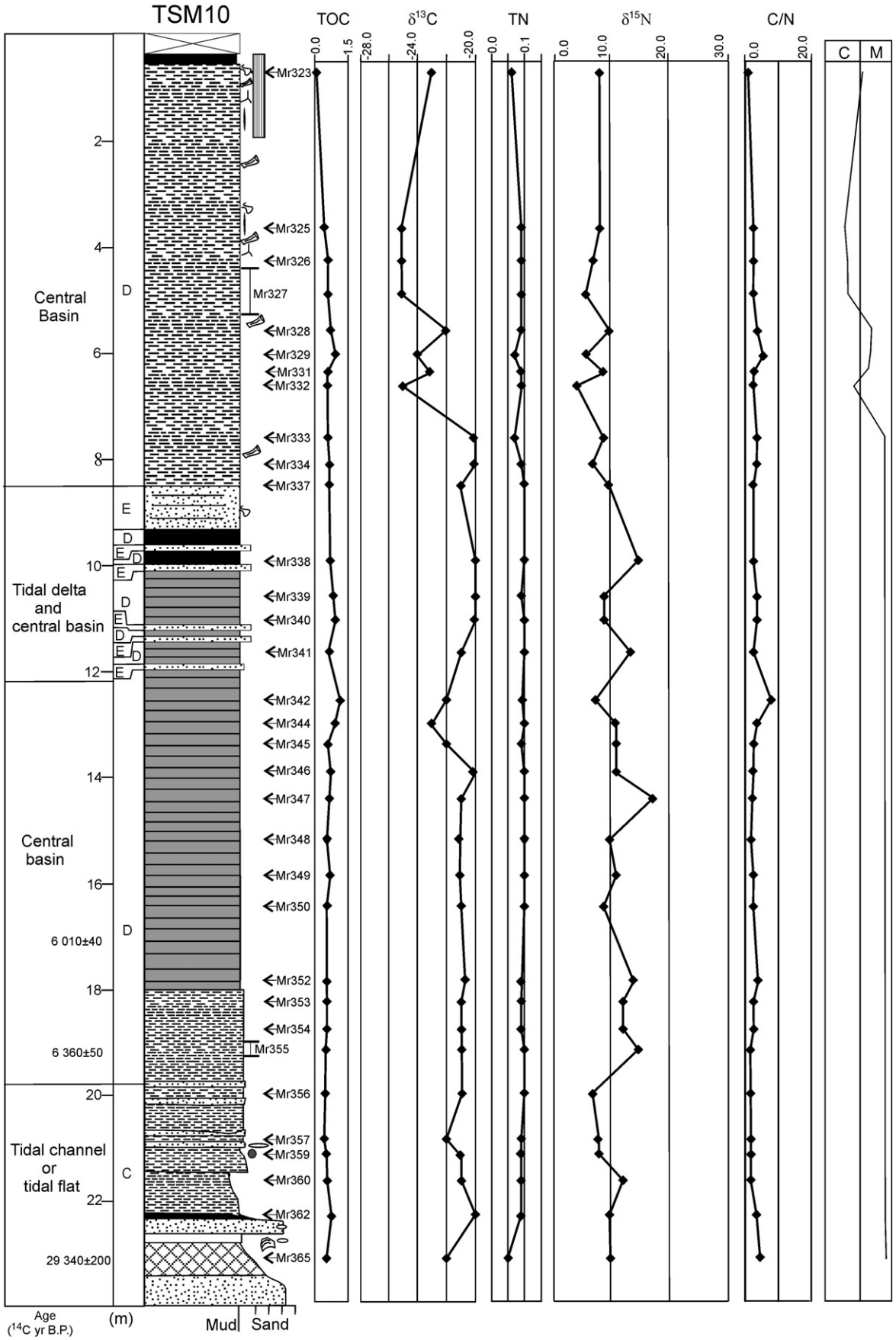

Fig. 3. Lithostratigraphic profile from TSM10, illustrating facies and facies associations, as well as the position of the analyzed samples with their respective $\delta^{13}C$, $\delta^{15}N$, TOC (total organic carbon), TN (total nitrogen), C/N values, and the interpretation of marine (M) or continental (C) influence. See Fig. 2 for legend.

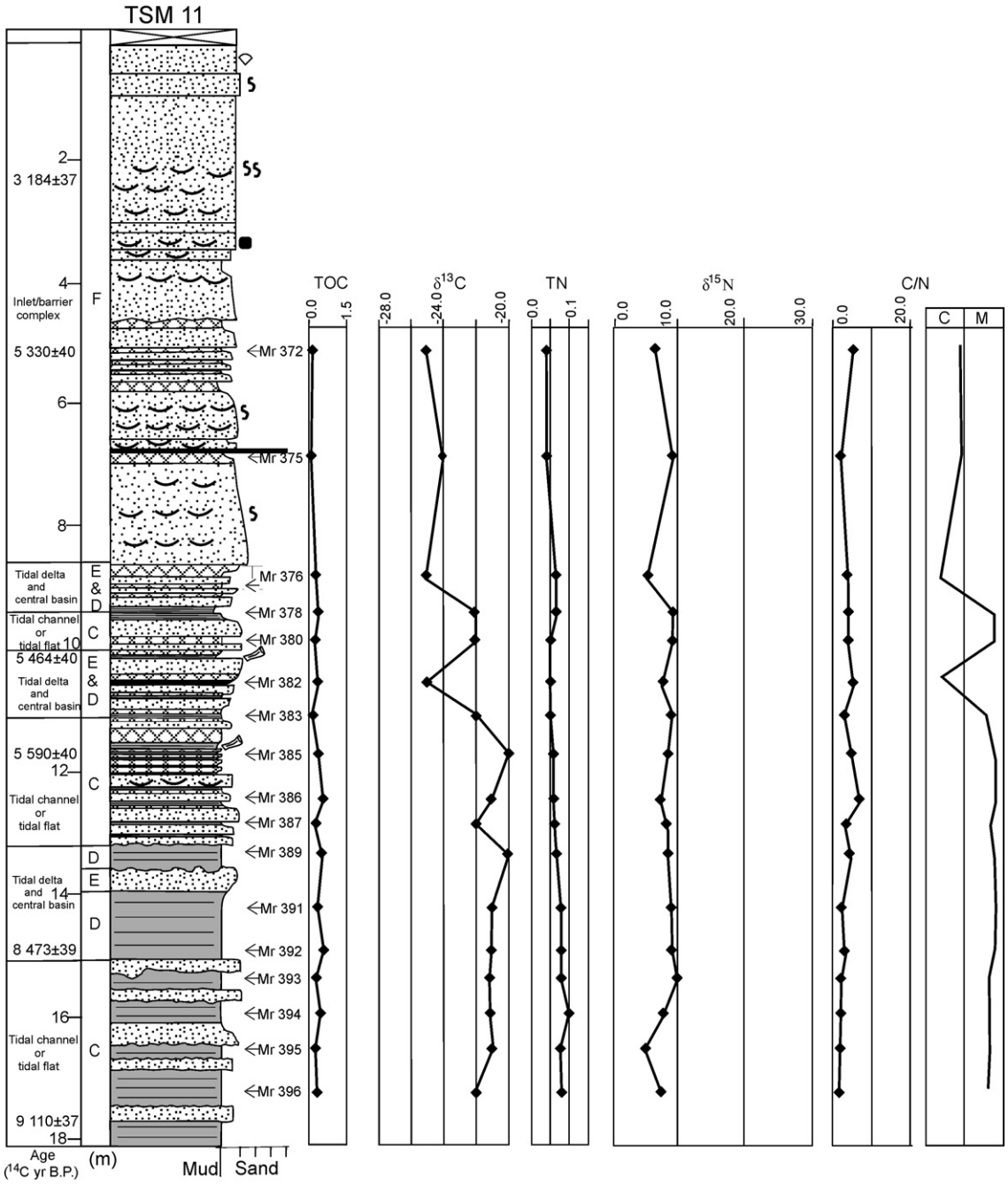

Fig. 4. Lithostratigraphic profile from TSM11, illustrating facies and facies associations, as well as the position of the analyzed samples with their respective $\delta^{13}C$, $\delta^{15}N$, TOC (total organic carbon), TN (total nitrogen), C/N values, with the interpretation of marine (M) or continental (C) influence. See Fig. 2 for legend.

elemental values that do not differ much from the previous association C, with $\delta^{13}C = -25.8$ to $-19.7‰$ (mean $= -22.6‰$); $\delta^{15}N = +4.7$ to $+14.8‰$ (mean $= +9.3‰$); C/N = 2.3 to 8.30 (mean = 5.0).

5.5. Facies association E (tidal delta)

This association occurs in TSM4, TSM10 and TSM11 (Figs. 2–4), being recorded between 8.1–10.0 m (TSM4) and 8.4–9.1 m (TSM10), 8.4–9.1 m, 9.9–11.0 m and 13.6–15.0 m (TSM11). In contrast to facies association D, these deposits are dominantly sandy, consisting of massive (facies Sm) or, less commonly, parallel laminated, fine- to very fine-grained sands (facies Sp). This association grades downward into heterolithic deposits (facies Hf, Hls and Hw) of facies association D, with thickening and coarsening upward successions. Plants debris and overload structures are locally present. Facies association E is characterized by carbon isotope values, in general, slightly lighter than facies association C and D, indicated by a narrower range of $\delta^{13}C$ variation between -25.7 and $-22.5‰$, with a mean of $-23.6‰$. Similarly, the nitrogen values also shows a slightly narrower range of variation relative to those associations between $\delta^{15}N = +5.3$ and $+9.4‰$, with a higher mean of $+7.7‰$). On the other hand, the C/N values display a narrower range of variation with respect to facies associations C and D, from values between 4.4 and 5.4, with a mean of 5.1.

5.6. Facies association F (tidal inlet/sand barrier)

This association was recorded only in TSM11 (located in the distal part of the paleoestuary), where it occurs above 8.4 m (Fig. 4).

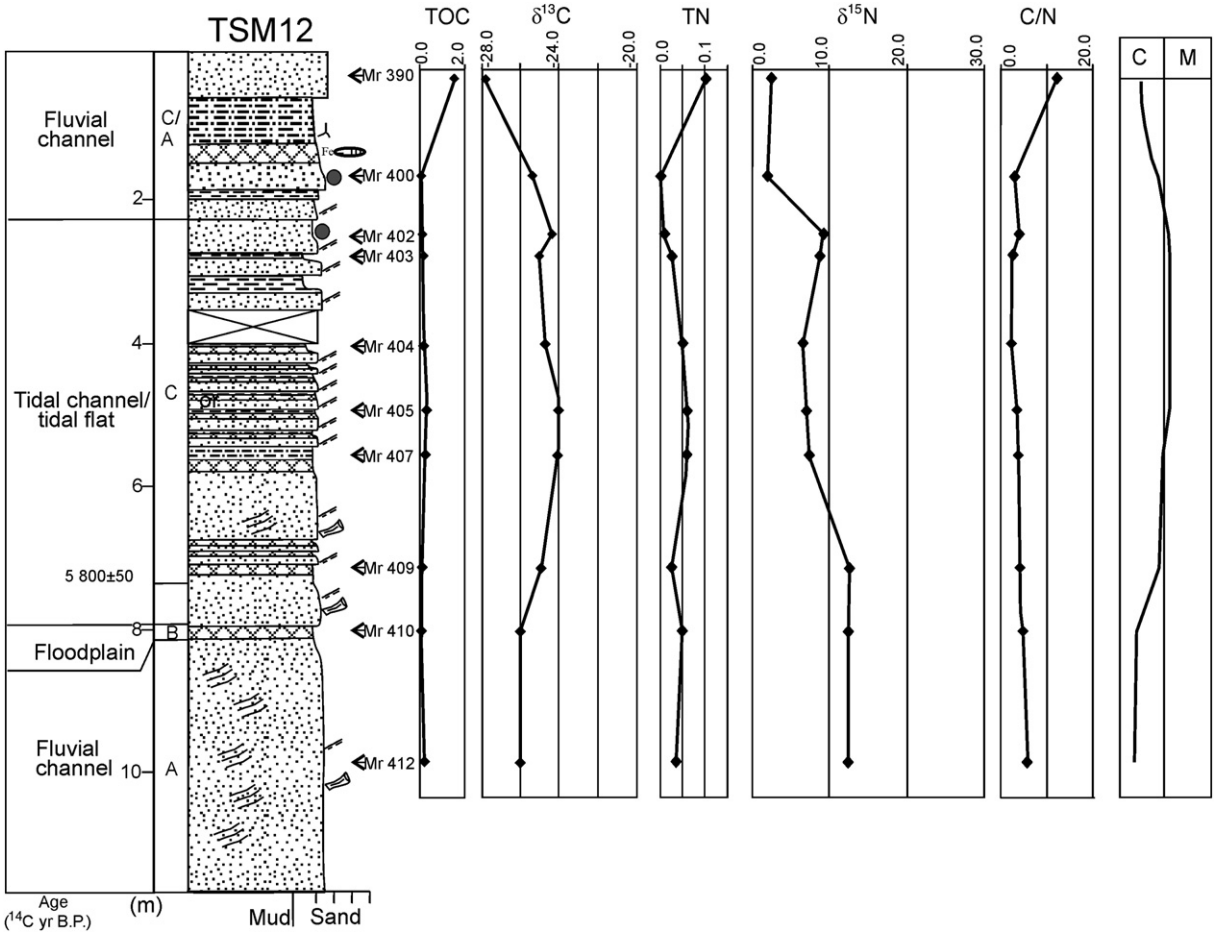

Fig. 5. Lithostratigraphic profile from TSM12, illustrating facies and facies associations, as well as the position of the analyzed samples with their respective $\delta^{13}C$, $\delta^{15}N$, TOC (total organic carbon), TN (total nitrogen), C/N values, with the interpretation of marine (M) or continental (C) influence. See Fig. 2 for legend.

The deposits are dominantly flaser heterolithic deposits (facies Hf) interbedded with fine- to very fine- and, less commonly, medium-grained, either massive (facies Sm) or cross-stratified (facies Sc) sands. Fragmented plant debris (*coffee-ground*) are frequent throughout this association. Except for the uppermost 3 m, the deposits are organized into erosive, sharp-based, fining upward successions that are up to 1.8 m thick, some of them ending upward into thin (>0.2 m thick) layers of lenticular/streaky (facies Hls) and wavy (Hw) heterolithic deposits. Undetermined trace fossils are disperse in the uppermost 8.5 m of this association, increasing in abundance in the uppermost 2.5 m, where there are iron-cemented, branched trace fossils, probably related to *Ophiomorpha*(?). These uppermost deposits also contain archeological pottery artifacts, which increase in abundance near the surface. This facies association display $\delta^{13}C = -25.8$ to -24.5‰, with a mean of 25.2‰, which is similar to the one from facies associations A and B. The $\delta^{15}N$ values are between $+6.5$ and $+9.9$‰, being closer to range of variation observed in facies association E, but with a mean of $+8.2$, which is approximately similar to the values obtained from all the other facies associations. On the other hand, the C/N = 3.7 to 6.7 are close to the range of variation obtained in associations C, D and E than in associations A and B. The difference of association F and the other associations is also reflected by the C/N mean of 5.2, which is much lower than the values obtained in associations A and B.

6. Paleoenvironmental interpretation

In addition to sedimentary facies characteristics, the paleoenvironmental interpretation presented below was based on results derived from elemental and isotope data. In general, there is an overall agreement that the $\delta^{13}C$ remains relatively constant in sediments (e.g., Thornton and McManus, 1994; Middelburg and Nieuwenhuize, 1998; Cloern et al., 2002, see also several references in Lamb et al., 2006 and Chen et al., 2008). However, degradation of organic matter might cause either a depletion or enrichment of ^{15}N (e.g., Saino and Hattori, 1980; Fry et al., 1991; Nakatsuka et al., 1997; Sachs and Repeta, 1999; Lehmann et al., 2002) due to the biosynthesis of inorganic nitrogen (e.g., Meyers, 1997; Chen et al., 2008). Therefore, one should be careful when including $\delta^{15}N$ and C/N in the interpretation of depositional environments. In the present study, this parameter was added to help the paleoenvironmental interpretation because of the assumed absence of terrestrial derived inorganic nitrogen in the analyzed samples. This assumption is supported by the analysis of TN versus TOC plot, as shown in Fig. 8. The graphic reveals good linear correlation between these elements, indicating nitrogen derivation from the organic matter, rather than from external inorganic sources.

The estuarine system previously identified using remote sensing was confirmed by facies analysis. This indicated an abundance of deposits formed in confined environments related to channels, which are interbedded with thick mud and heterolithic units originated by fluvial and tidal processes, as discussed in more detail below. Facies associations distinguished herein indicate depositional environments documented in many other estuarine successions recorded in the literature (e.g., Woodroffe et al., 1989; Dalrymple et al., 1992; Harris et al., 1992; Mulrennan and Woodroffe, 1998; Plink-Bjorklund, 2005; several papers in Dalrymple et al., 2006).

An estuarine interpretation of the morphological and facies data is consistent with the recorded $\delta^{13}C$, $\delta^{15}N$ and C/N values, which

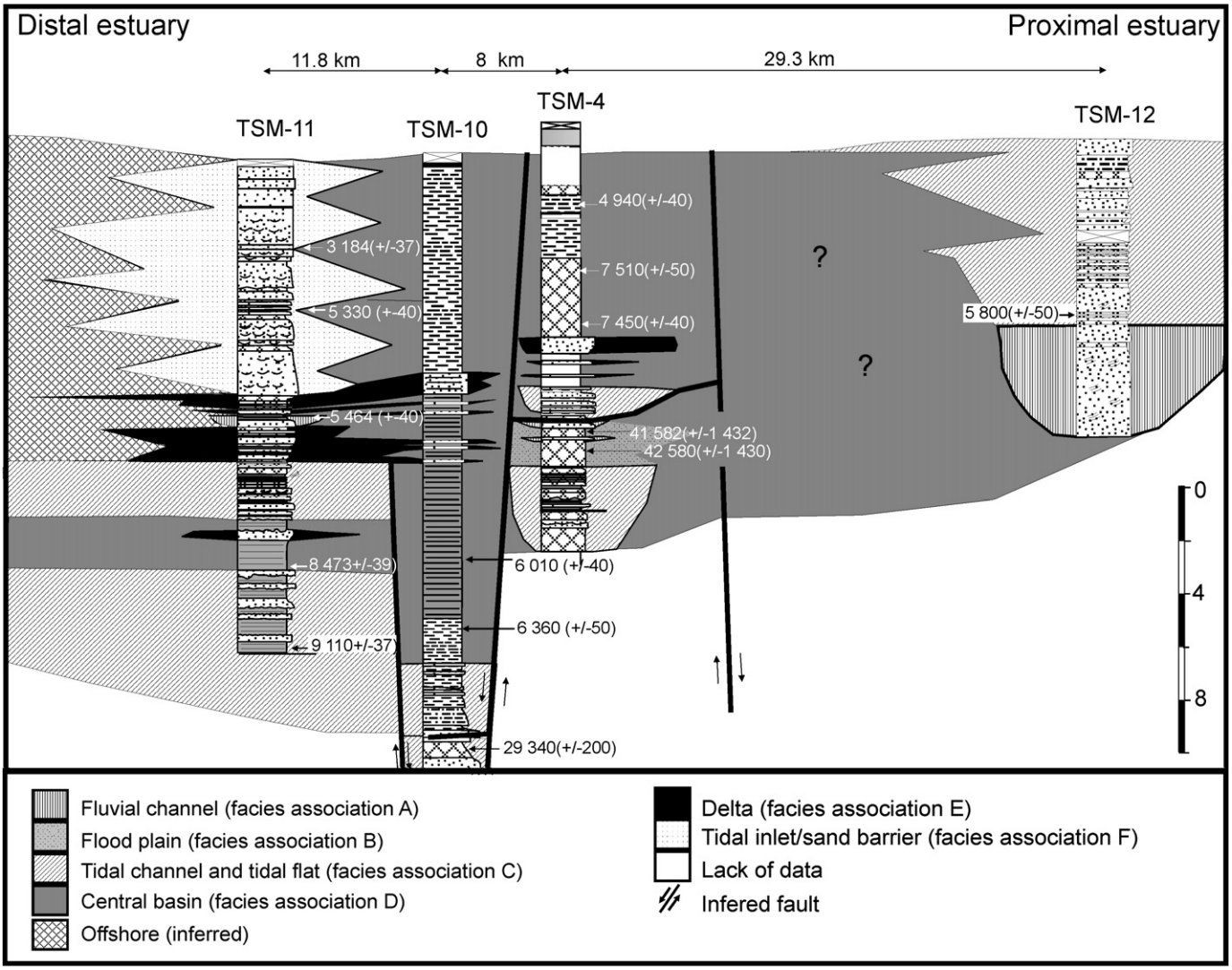

Fig. 6. Geological section derived from correlation of the studied lithostratigraphic profiles (see Fig. 1 for location). Faults are inferred in this section in order to better accommodate spatial facies variations. Vertical position of the profiles according to altitude.

suggests mixed sources of organic matter in the sediment, such as marine and freshwater phytoplankton, as well as terrestrial, as typical of estuaries (Fig. 9A,B). These values are also similar to those documented in many other estuarine systems (Salomons and Mook, 1981; Peterson et al., 1994; Thornton and McManus, 1994; Middelburg and Nieuwenhuize, 1998; Wilson et al., 2005a,b).

As expected, the isotope and C/N values do not show significant differences throughout the paleoestuary, because several facies associations are represented at each core. However, there is a consistent gradient in these values when individual facies associations are compared. The prevalence of sands in facies association A indicates a setting located nearby a sand source, with deposition close either to the proximal (i.e., fluvial-influenced) or distal (i.e., marine influence) portions of the estuary. The sharp and erosive base of these strata indicates high energy flows and erosion of pre-existing beds before sedimentation. The fining upward successions record decreasing flow energy through time. These features favor a channel setting as the most likely. Unfortunately, facies analysis based only on core data difficult to analyse the stratal architecture. However, comparison of the cores shows that facies association A, as well as most of facies association C, are laterally discontinuous, which is consistent with a channel setting. In general, Association A and B shows the lightest $\delta^{13}C$ values (Fig. 9A), which together with the relatively low C/N, suggest strong contribution of freshwater phytoplankton. However, the diagram with $\delta^{15}N/\delta^{13}C$ (Fig. 9B) indicates one sample in the marine-estuarine field, and two samples in the saltmarsh field, Together with facies characteristics, the isotopic and elemental data in association A point to settings with strong influence of fluvial inflows, but these were connected to the estuary, being momentaneously influenced by marine water. This interpretation is consistent with the fact that facies association A and B only occur in cores TSM12 and TSM4, located in the channelized proximal and marginal estuarine areas, respectively. The prevalence of muddy sediments in facies association B indicates sediment accumulation mostly from suspensions in a low energy paleoenvironment. The textural characteristics of this facies, together with the fact that these strata grade into fluvial-influenced channel deposits in fining upward successions, suggests that facies association B reflects floodplain deposits. As with association A, these deposits contain organic matter derived mostly from freshwater phytoplankton.

Facies association C displays sedimentological features that are similar to association A, suggesting deposition also within channels. However, the cross strata with frequent reactivations mantled by mud

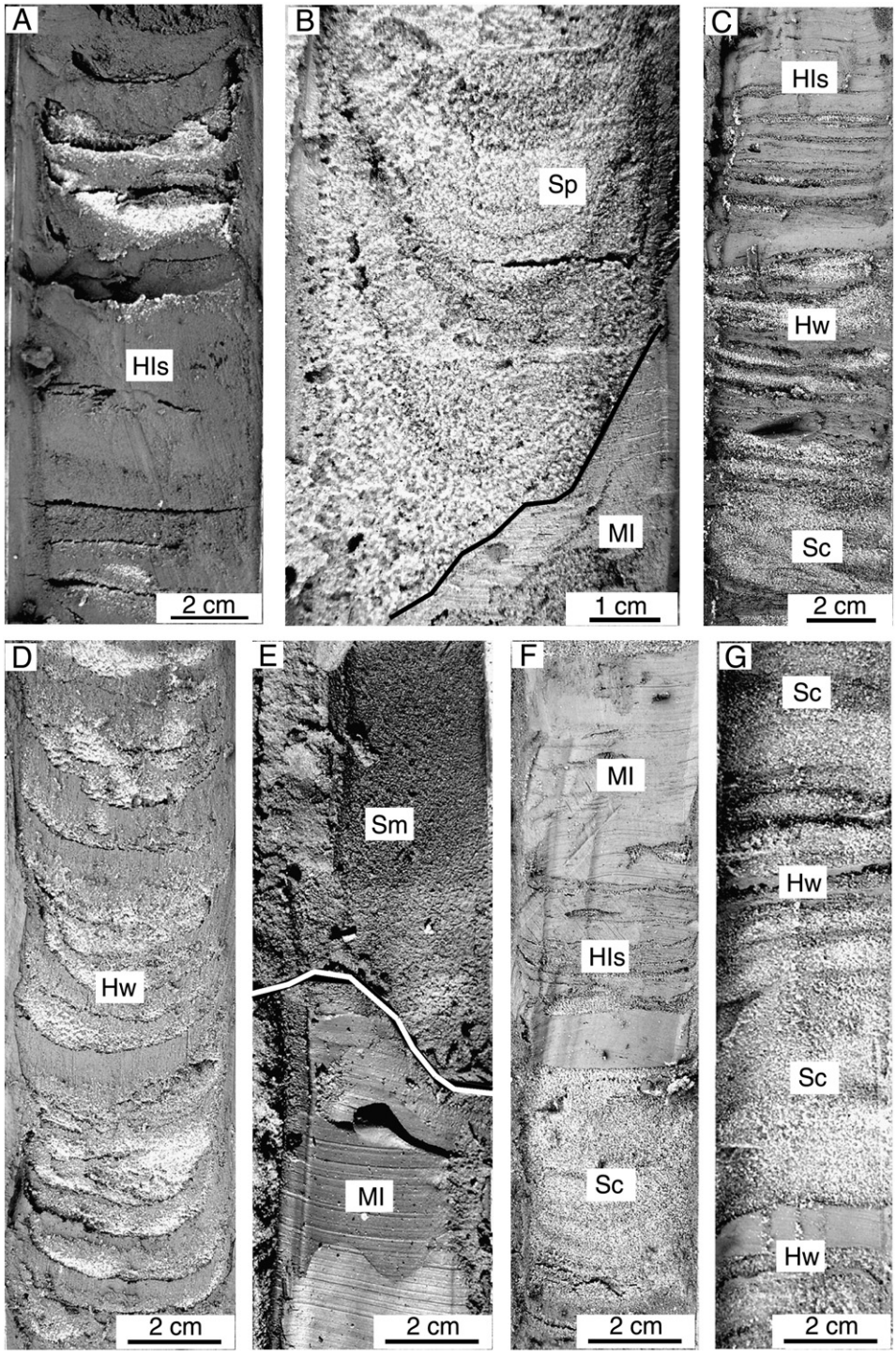

Fig. 7. Examples of sedimentary facies of the paleoestuarine deposits, illustrating: A) Lenticular/streaky heterolithic bedding (facies Hls). B) Laminated mud (facies Ml) cut down by an erosional surface (black line) overlain by parallel laminated sand (facies Sl), locally deformed during core sampling. C) Upward gradation from cross-laminated sand (facies Sc) to wavy (facies Hw) and lenticular/streaky (facies Hls) heterolithic beddings. D) Continuous wavy heterolithic bedding (facies Hw). E) Massive sand (facies Sm) that cuts down on laminated mud (facies Ml), forming a sharp erosional surface (white line). F) Upward gradation from cross-laminated sand (facies Sc) to lenticular/streaky heterolithic bedding (facies Hlw) and laminated mud (facies Ml), forming a fining upward succession. G) Cross-laminated sand (facies Sc) alternated with wavy heterolithic bedding (facies Hw). (In all figures, light gray tones = sand and dark gray tones = mud).

drapes and/or mud intraclasts, though not diagnostic, are suggestive of tidal currents (Terwindt and Breusers, 1972; Mowbray, 1983). Tidal currents are highly oscillatory flows that naturally result in sand deposition from traction during flood and ebb tides, which alternate with mud deposition from suspensions during slackwater periods. This process may produce cross-stratified sands with abundant mud drapes, as recorded in facies association C. Mud drapes are eventually reworked during tidal action, producing mud intraclasts. The $\delta^{13}C$, $\delta^{15}N$ and C/N values suggest organic carbon derived from mixed sources, but with an unambiguous prevalence of marine phytoplankton. This is shown by the fact that all samples from this association were plotted in, or less commonly, very close to the marine field (Fig. 9A). The plot of these samples in the $\delta^{15}N/\delta^{13}C$ diagram (Fig. 9B) also shows a main concentration in or nearby the marine-estuarine

Table 2
Summary of facies associations, isotope and C/N values, with the proposed interpretation of the depositional environments.

Facies association	Facies description	Isotopic and C/N values/type of organic matter	Interpretation
A	Fine to medium-grained cross-stratified sand (facies Sc). Subordinately, massive sand (facies Mm). Presence of mud/sand clasts and carbonized plant remains. These deposits are arranged into sharply-bounded, fining and thinning upward cycles.	$\delta^{13}C = -27.8$ to 24.8‰ (mean = −25.8‰), $\delta^{15}N = +7.1$ to +12.7‰ (mean = +7.10‰), C/N = 8.0 to 13.0 (mean = 11). Prevalence of freshwater phytoplankton, with only local contribution of marine phytoplankton.	Fluvial dominated channel
B	Massive muds (facies Mm), alternated with lenticular to streaky (facies Hls) and wavy (facies Hw) heterolithic deposits forming fining upward succession. Interbedded with association B	$\delta^{13}C = -28.1$ to −23.6‰ (mean = −26.0‰); $\delta^{15}N = +5.8$ to +11.8‰ (mean = +8.3‰); C/N = 5.2 to 14.5 (mean = 10.9). Mostly terrestrial plants and freshwater phytoplankton.	Floodplain
C	Fine to medium-grained, cross-stratified (facies Sc) or massive (Sm) sands interbedded with lenticular to streaky (facies Hls), wavy (facies Hw) and, locally, flaser (facies Hf) heterolithic deposits that are interbedded with massive mud (Mm), laminated mud (Ml) and massive pelite (facies Pm). Either tabular or erosional-based, fining upward successions.	$\delta^{13}C = -25.0$ to −19.7‰ (mean = −22.6‰); $\delta^{15}N = +5.4$ to +14.8‰ (mean = +9.0‰); C/N = 3.4 to 10.2 (mean = 5.1). Mixed sources, but with an unambiguous prevalence of marine phytoplankton contribution.	Tidal/plain channel
D	Massive (facies Mm) or laminated (facies Mp) mud interbedded with massive pelite (facies Pm), as well a lenticular to streaky (facies Hls) and wavy (Hw) heterolithic deposits.	$\delta^{13}C = -25.8$ to −19.7‰ (mean = −22.6‰); $\delta^{15}N = +4.7$ to +14.8‰ (mean = +9.3‰); C/N = 2.3 to 8.3 (mean = 5.0). Mixture of organic matter derived mostly from marine phytoplankton, but with frequent influence of freshwater phytoplankton.	Central basin
E	Massive sand (facies Mm) or, less commonly, parallel laminated sand (facies Sp) interbedded with facies association D, forming coarsening and thickening upward successions.	$\delta^{13}C = -25.7$ to −22.5‰ (mean = −23.6‰); $\delta^{15}N = +5.3$ to +9.4‰ (mean = +7.7‰); C/N = 4.4 to 5.4 (mean = 5.1). Strong influence of marine organic carbon, but with freshwater and, locally, terrestrial contributions.	Tidal delta
F	Massive sand (facies Sm) and flaser bedded deposits (facies Hf), locally interbedded with lenticular heterolithic to streaky (facies Hls) and wavy (Hw) heterolithic beddings grading upward from facies association D.	$\delta^{13}C = -25.8$ to −24.5‰ (mean = −25.2‰); $\delta^{15}N = +6.5$ to +9.9‰ (mean = +8.2); C/N = 3.7 to 6.7 (mean = 5.2). Mixture of organic carbon derived from marine, freshwater phytoplankton	Tidal inlet/ sand barrier

setting. The prevalence of marine phytoplankton is suggested for the organic matter within muddy and heterolithic deposits that grade into tidal channel deposits of facies association C. These characteristics led to relate these fine-grained deposits to tidal flats. Tidal flats are abundant in estuaries due to the increment of the tidal prism within coastal embayments.

Facies association D records a setting with the lowest energy in this depositional system, as recorded by mud packages up to 8 m thick. This, together with the fact that these deposits occur in almost all the analyzed cores (except TSM12), point to a catchment basin of considerable size. The relation of $\delta^{13}C$ and C/N, combined with the $\delta^{15}N/\delta^{13}C$ diagram, suggest organic matter derived mostly from marine phytoplankton, with less influence of freshwater contribution. Within the proposed estuarine model, facies association D is related to a central basin setting. Many estuaries are associated with distal barriers. In these cases, the central estuary is confined giving rise to an enlarged basin. Marine and fluvial flows progressively lose energy toward this central basin, which is a site favorable for mud accumulation (Nichols et al., 1991; Barusseau et al., 1985; Reinson, 1992). Due to its location in the central estuary, central basin sediments contain organic matter derived from either marine or freshwater phytoplankton.

Facies association E is related to sand deposition through suspension lobes within a confined basin, as suggested by the arrangement into thickening upward packages due to increased flow energy through time, and the interbedding with facies association D. Estuarine central basins receive sands derived from either marine or fluvial environments, which results in deposition of tidal deltas and bayhead deltas, respectively. Many estuarine central basins documented in the literature contain similar deposits (e.g., Sha and de Boer, 1991; Nichols et al., 1991; Dalrymple et al., 1992). Similarly to facies association D, the integrated analysis of $\delta^{13}C$, $\delta^{15}N$ and C/N values in association E reveal strong influence of marine organic carbon, but with contributions of freshwater phytoplankton (Fig. 9A,B). The overall prevalence of marine-derived organic matter in the sandy lobes is consistent with tidal deltas. The local (e.g., 8.4–9.1 m, and 9.9–11.0 m of TSM11) presence of organic matter derived from freshwater phytoplankton might record the mixing of fluvial inflow on bayhead deltas.

Facies association F is related to tidal inlet/sand barrier, an interpretation consistent with the sandy nature of the facies, with an arrangement of sharp-based, fining upward cycles, and location confined to distal estuarine areas (i.e., TSM11). The bioturbated deposits with archeological remains that occur above 2.5 m might record part of a sand barrier. The abundance of bioturbation over these strata, with possible *Ophiomorpha*, although not exclusive, is a common feature in tidal influenced environments. The presence of tidal inlet, together with deltas and central basin deposits, conform to the occurrence of a barrier at the estuary mouth. The $\delta^{15}N$, $\delta^{13}C$ and C/N data derives only from two samples, which constrain their use for paleoenviromental purposes. However, it is noteworthy that these samples also indicate a mixture of organic carbon derived from marine and freshwater phytoplankton, as expected in environments associated with barrier complexes.

7. Discussion

7.1. A wave-dominated estuarine morphology

The integrated approach applied in this work confirms the occurrence of a large estuarine system in northeastern Marajó Island during the Late Pleistocene and Holocene. The increased fluvial influence towards TSM12 suggests that the estuary was fed by continental influxes derived from the east/southeast portions of the island. This proposition is consistent with the recorded funnel-shaped paleoestuarine morphology that progressively narrows in this direction, where it grades into a meandering paleochannel that is suddenly interrupted at the island edge (Rossetti et al., 2007). According to these authors, a continental fluvial inflow was active when Marajó Island was still connected to mainland. This flow was interrupted during the island detachment during the Holocene.

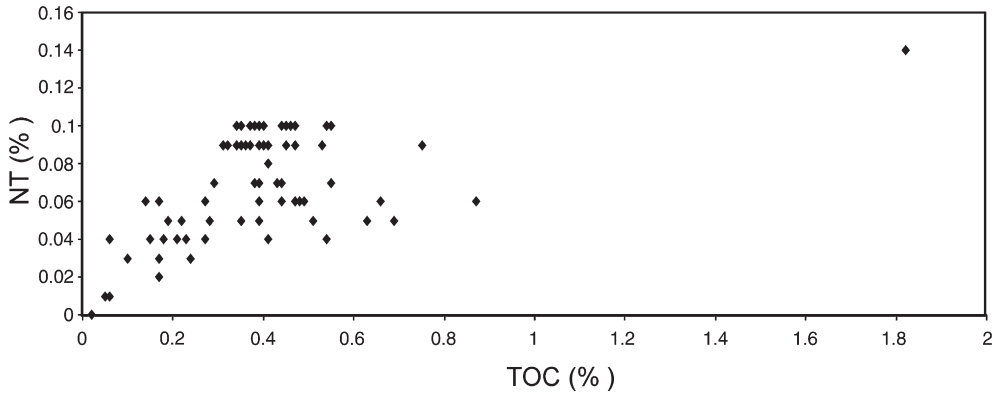

Fig. 8. Diagram with total organic carbon (TOC) versus total nitrogen (TN) for all analyzed samples. Note the linear correlation between these values.

Funnel-shaped estuaries, as recorded in the study area, are often associated with tidal dominated coasts (Woodroffe et al., 1989; Dalrymple et al., 1992; Harris et al., 1992; Mulrennan and Woodroffe, 1998; Plink-Bjorklund, 2005), a model consistent with the modern macrotidal-dominated northern Brazilian coast. However, facies associations recognized in the study area suggest a paleoestuary with tidal inlet/sand barrier, central basin and deltas. These characteristics more likely conform to the geometry expected in wave-dominated estuaries (Frey and Howard, 1986; Dalrymple et al., 1992; Fig. 10). Some elongated estuaries similar to the ones developed along tide-dominated coasts may contain a variety of sub-environments typical of wave-dominated coasts, as exemplified by the Gironde Estuary (Allen and Posamentier, 1993). However, in addition to tidal currents and waves, a number of other factors might define the estuarine morphology, including the history of the previous drainage, nature of the substratum, subsidence rate, sea-level change and sediment supply (Ricketts, 1991). Further research is necessary to determine which of these factors might have contributed to the development of a funnel-shaped estuary with the central basin and the associated tidal inlet/sand barrier of the study area.

7.2. Sea-level history

The stratigraphic correlation (Fig. 6) reveals the coexistence of fluvial channel, floodplain, tidal channel and/or tidal flat settings indicating the establishment of an estuarine system around 42,000 yr B.P. The presence of this estuary implies in a rise in relative sea level. After 29,340 ($\pm$200) ^{14}C yr B.P., there was a period of relative sea level fall, when the estuary was abandoned and the previously deposited sediments were eroded, as recorded by a discontinuity surface.

Following a period of fall, northeastern Marajó Island experienced a relative sea level rise (transgressive phase) in the early Holocene dated at 9110 $\pm$ 37 ^{14}C yr B.P., which led to the return of estuarine deposition. Sea level continued to rise until around 5464 $\pm$ 40 ^{14}C yr B.P, a process that resulted in the superposition of tidal channel and tidal flat on fluvial-influenced deposits in the proximal estuary (TSM12). During this time, the central basin was expanded, resulting in a thick mud succession, which is well documented in TSM10. Tidal deltas formed in association to barrier islands, which resulted in sand deposition within central basin settings (TSM11 and TSM10).

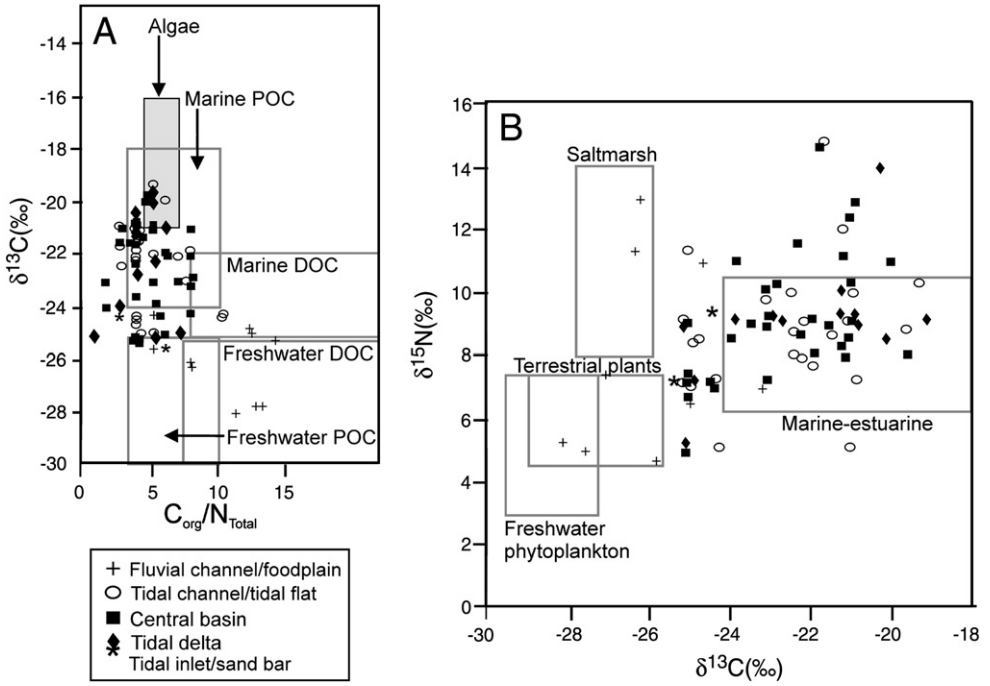

Fig. 9. Diagrams illustrating the relationship between δ^{13}C and C/N (A) and δ^{15}N and δ^{13}C (B) values of the studied sediments, with interpretation according to data presented by Middelburg and Nieuwenhuize (1998), Cloern et al. (2002), Ogrinc et al. (2005). (DOC = dissolved organic carbon; POC = particulate organic carbon).

The fluvial inflow was cut off sometime between the early to middle Holocene, while the relative sea level might have continued to rise. The relative sea-level stabilized and started to fall after nearly 5464 ± 40 ^{14}C yr B.P. During this evolutionary stage, mud deposition in the central basin areas continued (TSM10). In this core, marine-derived organic carbon was recorded at least up to 1 m depth. This suggests a marine connection until recently, when the area became dominated by lacustrine sedimentation with the development of Lake Arari.

7.3. Controlling mechanisms

The recorded relative sea level history and the consequent evolution of a compound paleoestuary in the study area might be related to the combination of eustasy and tectonics. The analyzed sedimentary succession indicating that estuarine conditions had been established at least around 42,000 ka B.P. This implies the presence of a transgressive event sometime before and/or around this time, as estuaries are essentially transgressive depositional settings. This period coincides with the progressive drop in sea level that followed the last interglacial time interval (Fig. 11). Therefore, relating the development of this estuary solely due to global sea level seems to be highly implausible, unless it is a reflection of a punctuated transgression superposed upon the overall sea level drop. Noteworthy is that there is no record of a Late Pleistocene transgression other than the Penultimate or Cananéia Transgression (Martin et al., 1982, 1986; Tomazelli and Dillenburg, 2007) in other areas of the Brazilian territory, which corresponds to the Last Interglacial Maximum that extended from nearly 118–130 ka B.P. (Lambeck and Nakada, 1992; Stirling et al., 1995).

The relative sea level fall recorded between 29,000 and 9000 yr B.P. took place contemporaneously to two glacial episodes, the Last Glacial Maximum and the Younger Dryas, which occurred between 25,000–18,000 yr B.P. and 12,600–11,800 yr B.P., respectively (e.g., Crowley and North, 1991). Palynological data show that other areas of Brazilian Amazonia record these events (e.g., Van der Hammen et al., 1992; Van der Hammen and Absy, 1994; Latrubesse and Rancy, 1998). A climate relatively more arid than the present one is recorded until, at least, 11,300 ^{14}C yr B.P. in central Amazonia (Rossetti et al., 2005). Thus, it is likely a relationship between the relative sea level fall in the study area and the occurrence of the Last Glacial Maximum and the Younger Dryas stadial. Similarly, the data presented herein shows a transgression from 9110 ± 37 ^{14}C yr B.P. to around 5464 ± 40 ^{14}C yr B.P. This was the time when the Younger Dryas ice sheets melted, which produced a rise in sea level. However, the transgressive peak associated with this event is usually indicated to have occurred in the mid Holocene, when sea level reached around 5 m above the modern one (e.g., Shackleton, 1988). Therefore, there is a little offset in the events when the global curve is compared to the history of sea level change in Marajó Island, as the transgressive peak in this area seems to have taken place in the early to mid Holocene, with stabilization and beginning of a fall sometime around 5464 ± 40 ^{14}C yr B.P. This interpretation is consistent with records from other Brazilian areas, where a rise in sea level has been proposed until approximately 7 ka B.P., with stabilization between 7 and 5 ka B.P. (Milne et al., 2005; Suguio et al., 1985; Martin et al., 1986). This pattern is also compatible with many studies undertaken in other areas of Northern Brazil (Behling and Costa, 2000, 2001; Behling, 2001; Behling et al., 2001a,b; Souza-Filho and Paradella, 2003; Cohen et al., 2004, 2005a,b; Vedel et al., 2006).

The mid to late Holocene relative sea level drop reconstructed from Marajó Island is in agreement with the overall worldwide drop in sea level to its modern position since the mid Holocene rise. This interpretation also conforms with the statement that the late Holocene sea level in Southern Brazil was only less than 1 m above the modern one (e.g., Angulo and Lessa, 1997; Lessa and Angulo, 1998; Angulo et al., 2006). However, with a few exception (i.e., Toledo and Bush, 2008), the present data conflict with the late Holocene sea-level history reconstructed from other areas in Northern Brazil, where an overall rise has been proposed after a brief mid Holocene fall (Behling and Costa, 2000, 2001; Behling, 2001; Behling et al., 2001a,b; Souza-Filho and Paradella, 2003; Cohen et al., 2004, 2005a,b; Vedel et al., 2006). In addition, there are records of late Holocene sea level rises up to 3 to 4 m above the modern one in Northeastern Brazil (e.g., Suguio et al., 1985; Martin et al., 1986; Bezerra et al., 2003).

Differences in sea level behavior, as detected among several localities of the Brazilian territory, have been related to tectonic influence (Martin et al., 1986; Angulo and Suguio, 1995). In fact, an increasing volume of publications has demonstrated the significance of tectonics in the development of Quaternary sedimentary successions in Brazil (Costa et al., 2001; Bezerra and Vita-Finzi, 2000; Bezerra et al., 2003; Rossetti et al., 2008a,b). A few other works have suggested that episodes of eustatic rises along the South American plate during the Quaternary were enhanced by subsidence due to post-rifting tectonic reactivations (Morais-Neto and Alkmin, 2001; Barreto et al., 2002; Bezerra et al., 2001).

The importance of tectonics related to fault reactivation in Marajó Island has been also addressed in several publications, including its role in the preservation of Quaternary sediments (Costa et al., 2002; Rossetti and Valeriano, 2007; Rossetti et al., 2007). Tectonic activity

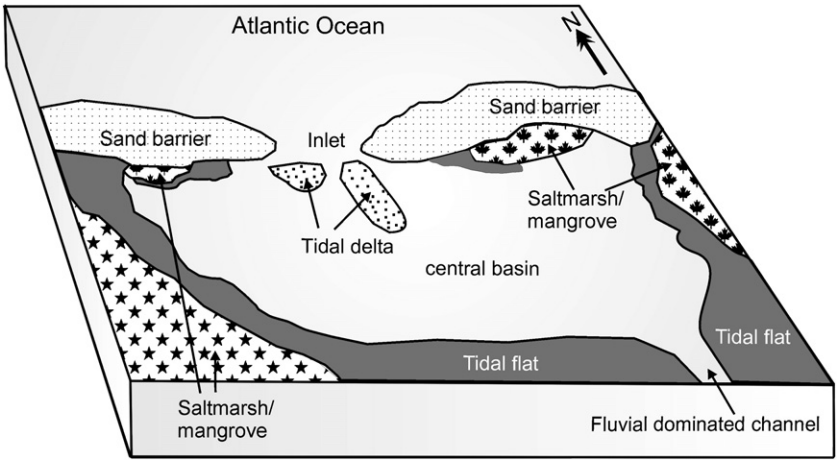

Fig. 10. A cartoon illustrating the wave-dominated depositional system proposed for the studied deposits in eastern Marajó Island from Late Pleistocene until the early/middle Holocene. (Depiction of saltmarsh and mangrove environments shown only as illustration for completing the model, as these deposits could not be distinguished from muddy central basin deposits in this study).

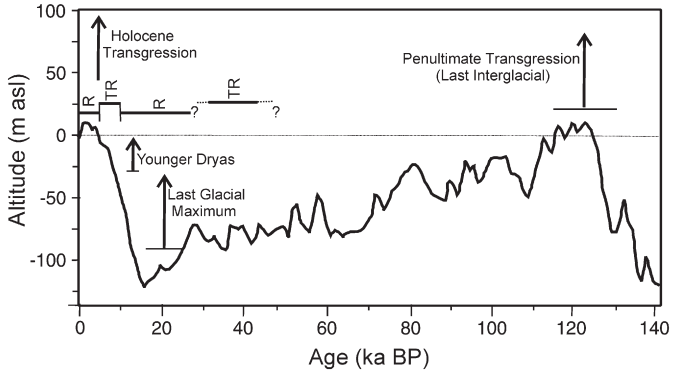

Fig. 11. Global sea level curve since the last interglacial period based on oxygen isotopes from Shackleton (1988), and main transgressive–regressive episodes recognized in Marajó Island (R = regression; TR = transgression; see text for further explanation).

during the Quaternary, and also Tertiary, in Northern Brazil has been related to reactivation of faults formed during the origin of the marginal basins as a consequence of the South Atlantic rifting (e.g., Szatmari et al., 1987; Aranha et al., 1990; Costa and Hasui, 1997; Azevedo, 1991). An earlier study has presented evidence suggesting that the origin and evolution of the analyzed paleoestuary was triggered by tectonic activity (Rossetti et al., 2008b). The stratigraphic correlation of the studied cores presented herein (Fig. 6) is consistent with this hypothesis. Fault activity is indicated by vertical displacements of correlatable strata of more than 10 m. Where deposits of same ages are located in a deeper position, the sedimentary column is thicker, suggesting depocenters with higher sedimentation rates. This stratal distribution can be better explained through fault displacements taking place simultaneously with sediment deposition. According to previous proposition, eastern Marajó Island was undergone to a slight subsidence during the latest Quaternary (Rossetti and Valeriano, 2007; Rossetti et al., 2008a).

Based on the foregoing discussion, there is a possibility to relate changes in sea level in Marajó Island to tectonics. For instance, the transgression recorded around 42,000 ka B.P. could be due to tectonic subsidence, instead of punctuated rises in eustatic sea level superimposed on the overall post-interglacial sea level drop, as previously discussed. The reported subsiding nature of eastern Marajó during the latest Quaternary is consistent with this interpretation. Considering this tectonic framework, the offset in the Holocene transgressive peak with respect to the global curve, as detected in Marajó, could also be attributed to a tectonic interference. Despite that the progressive late Holocene sea level drop recorded in this study area matches with a eustatic lowering, it is worthwhile to recall that these data conflict with interpretations from other areas in Northern and Northeastern Brazil, where several rises in sea-level have been reported in this time length. This shows that much further efforts are still needed in order to establish a more precise late Quaternary sea level chronology in Brazil.

8. Conclusions

Facies, ^{14}C dating, $\delta^{13}C$, $\delta^{15}N$, C/N analyses of late Quaternary estuarine deposits collected from core data in Marajó Island furnished new information for evaluating whether isotope and geochemical methods can be used for helping characterizing and reconstructing the evolution of estuarine systems through time. The integrated approach provided in this paper confirmed the presence of a paleoestuarine system in Marajó Island, and allowed analysis of the distribution of stratal patterns within the context of relative sea level fluctuations. The data presented herein lead to suggest that changes in sea level in Northern Brazil might be related, not only to global fluctuations, but also to tectonic motion promoted by post-rifting tectonic reactivations. This is suggested because the sea level fluctuations recognized in the study area are not all coincidental with the eustatic pattern. For instance, the initial estuarine transgression before nearly 29,000 yr B.P. occurred simultaneous to the major tendency of eustatic drop that followed the last interglacial. In addition, the main Holocene transgression in Marajó is recorded between nearly 9 to 5 ka B.P., while worldwide this transgression peaks at the mid Holocene, when relative sea level in Marajó started to stabilize leading to significant coast progradation. This divergence in sea level behavior with respect to the global pattern, combined with the increased record of late Pleistocene and Holocene tectonic activity in this region, led to hypothesize that these transgressive events might have been triggered by tectonic subsidence, rather than eustasy.

Acknowledgments

This work was funded by FAPESP (Project # 004/15518-6), with the logistic contribution of the Goeldi Museum and the Mayor of the town of Santa Cruz do Arari. The first and second authors hold a scholarship from CAPES, and a research grant from CNPq, respectively. These acknowledgements are extensive to two anonymous reviewers for the numerous suggestions that helped to improve significantly the early version of this manuscript.

References

Allen, G.P., Posamentier, H.W., 1993. Sequence stratigraphy and facies model of an incised valley fill; the Gironde Estuary, France. J. Sediment. Res. 63, 78–391.
Angulo, R.J., Lessa, G., 1997. The Brazilian sea level curves: a critical review with emphasis on the curves from Paranaguá and Cananéia regions. Mar. Geol. 140, 141–166.
Angulo, R.J., Suguio, K., 1995. Re-evaluation of the maxima of the Holocene sea-level curve for the State of Paraná, Brazil. Palaeogeogr. Palaeoclimat. Palaeoecol. 112, 385–393.
Angulo, R.J., Lessa, G.C., Souza, M.C., 2006. A critical review of mid- to late-Holocene sea-level fluctuations on the eastern Brazilian coastline. Quat. Sci. Rev. 25, 486–506.
Aranha, L.G.F., Lima, H.P., Souza, J.M.P., Makino, R.K., 1990. Origem e evolução das bacias de Bragança-Viseu, São Luís e Ilha Nova. In: Gabaglia, G.P., Milani, E.J. (Eds.), Origem e Evolução das Bacias Sedimentares. Petrobras, Rio de Janeiro, pp. 221–232.
Azevedo, R.P., 1991. Tectonic evolution of Brazilian equatorial continental margin basins. PhD Thesis, University of London, London.
Barreto, A.M.F., Bezerra, F.H.R., Suguio, K., Tatumi, S.H., Yee, M., Paiva, R., Munita, C.S., 2002. Late Pleistocene marine terrace deposits in northeastern Brazil: sea-level changes and tectonic implications. Palaeogeogr. Palaeoclimat. Palaeoecol. 179, 57–69.
Barusseau, P., Diop, E.H.S., Saos, J.L., 1985. Evidence of dynamics reversal in tropical estuaries, geomorphological and sedimentological consequences (Salum and Casamance Rivers, Senegal). Sedimentology 32, 543–552.
Behling, H., 2001. Late Quaternary environmental changes in the Lagoa da Curuça region (eastern Amazonia, Brazil) and evidence of Podocarpus in the Amazon lowland. Vegetation Hist. Archaeobot. 10, 175–183.
Behling, H., Costa, M.L., 2000. Holocene environmental changes from the Rio Curuá record in the Caxiuanã region, eastern Amazon Basin. Quat. Res. 53, 369–377.
Behling, H., Costa, M.L., 2001. Holocene vegetational and coastal environmental changes from the Lago Crispim record in northeastern Pará State, eastern Amazonia. Rev. Palaeobot. Palynol. 114, 145–155.
Behling, H., Cohen, M.C.L., Lara, R.J., 2001a. Studies on Holocene mangrove ecosystem dynamics of the Bragança pensinsula in northeastern Pará, Brazil. Palaeogeogr. Palaeoclimatol. Palaeoecol. 167, 87–101.
Behling, H., Keim, G., Irion, G., Junk, W., Mello, J.N., 2001b. Holocene environmental changes in the Central Amazon Basin inferred from Lago Calado (Brazil). Palaeogeogr. Palaeoclimatol. Palaeoecol. 173, 87–101.
Bezerra, F.H.R., Vita-Finzi, C., 2000. How active is a passive margin? Paleoseismicity in northeastern Brazil. Geology 28, 591–594.
Bezerra, F.H.R., Amaro, V.E., Vita-Finzi, C., Saadi, A., 2001. Pliocene-Quaternary fault control of sedimentation and coastal plain morphology in NE Brazil. J. South Am. Earth Sci. 14, 61–75.
Bezerra, F.H.R., Barreto, A.M.F., Suguio, K., 2003. Holocene sea level history on the Rio Grande do Norte State coast, Brazil. Mar. Geol. 196, 73–89.
Chen, F., Zhang, L., Yang, Y., Zhang, D., 2008. Chemical and isotopic alteration of organic matter during early diagenesis: evidence from the coastal area off-shore the Pearl River estuary, south China. J. Mar. Syst. 74, 372–380.
Cloern, J.E., Canuel, E.A., Harris, D., 2002. Stable carbon and nitrogen isotope composition of aquatic and terrestrial plants of the San Francisco Bay estuarine system. Limnol. Oceanogr. 47, 713–729.

Cohen, M.C.L., Lara, R.J., Szlafsztein, C.F., Dittmar, T., 2004. Mangrove inundation and nutrient dynamics under a GIS perspective. Wet. Ecol. Manag. 12, 81–86.
Cohen, M.C.L., Behling, H., Lara, R.J., 2005a. Amazonian mangrove dynamics during the last millennium: the relative sea-level and the Little Ice Age. Rev. Palaeo. Palynol. 136, 93–108.
Cohen, M.C.L., Souza-Filho, P.W.M., Lara, R.J., Behling, H., Angulo, R.J., 2005b. A model of Holocene mangrove development and relative sea-level changes on the Bragança Peninsula (Northern Brazil). Wet. Ecol. Manag. 13, 433–443.
Costa, J.B.S., Hasui, Y., 1997. Evolução geológica da Amazônia. In: Costa, M.L., Angélica, R. S. (Eds.), Contribuições à Geologia da Amazônia. Sociedade Brasileira de Geologia, Belém, pp. 15–19.
Costa, J.B.S., Bemerguy, R.L., Hasui, Y., Borges, M.S., 2001. Tectonics and paleogeography along the Amazon River. J. S. Am. Earth Sci. 14, 335–347.
Costa, J.B., Hasui, Y., Bemerguy, R.L., Soares Jr., A.V., Villegas, J., 2002. Tectonics and paleogeography of the Marajó Basin, northern Brazil. An. Acad. Bras. Ciênc. 74, 519–531.
Crowley, T.J., North, G.R., 1991. Paleoclimatology. Oxford University Press, Oxford New York. 339 pp.
Dalrymple, R.W., Zaitlin, B.A., Boyd, R., 1992. Estuarine facies models: conceptual basis and stratigraphic implications. J. Sediment. Petrol. 62, 1130–1146.
Dalrymple, R.W., Leckie, D., Tillman, R.W., 2006. Incised Valleys in Time and Space. SEPM Spec. Publ. 85.
Deines, P., 1980. The isotopic composition of reduced organic carbon. In: Fritz, P., Fontes, J.C. (Eds.), Handbook of Environmental Isotope Geochemistry. Gisewir, Amsterdam, pp. 329–406.
Frey, R., Howard, J.D., 1986. Mesotidal estuarine sequences: a perspective from the Georgia Bigth. J. Sediment. Petrol. 56, 911–924.
Fry, B., Sherr, E.B., 1984. ^{13}C measurements as indicators of caborn flow in marine and freshwater ecosystems. Contrib. Mar. Sci. 27, 15–47.
Fry, B., Jannasch, H.W., Molyneaux, S.J., Wirsen, C.O., Muramoto, J.A., King, S., 1991. Stable isotope study of the carbon, nitrogen and sulfur cycles in the Black Sea and the Cariaco Trench. Deep-Sea Res. 38, 1003–1019.
Graham, M.C., Eaves, M.A., Farmer, J.G., Dobson, J., Fallick, A.E., 2001. A study of carbon and nitrogen stable isotope and elemental ratios as potential indicators of source and fate of organic matter in sediments of the Forth Estuary, Scotland. Estuar. Coast. Shelf Sci. 52, 375–380.
Harris, P.T., Pattiaratchi, C.B., Cole, A.R., Keene, J.B., 1992. Evolution of subtidal sandbanks in Moreton Bay, eastern Australia. Mar. Geol. 103, 225–247.
Lajtha, K., Marshall, J.D., 1994. Sources of variation in the stable isotopic composition of plants. In: Michener, R.H., Lajtha, K. (Eds.), Stable Isotopes in Ecology and Environmental Science. Blackwell Scientific, Oxford, pp. 1–21.
Lamb, A.L., Wilson, G.P., Leng, M.J., 2006. A review of coastal palaeoclimate and relative sea-level reconstructions using $\delta^{13}C$ and C/N ratios in organic material. Earth-Sci. Rev. 75, 29–57.
Lambeck, K., Nakada, M., 1992. Constraints on duration of the Last Interglacial period and variations. Nature 357, 125–128.
Latrubesse, E.M., Rancy, A., 1998. The Late Quaternary of the Upper Juruá River, southwestern Amazonia, Brazil: geology and vertebrate paleontology. Quat. South Am. Antarct. Penins 11, 27–46.
Lehmann, M.F., Bernasconi, S.M., Barbieri, A., McKenzie, J.A., 2002. Preservation of organic matter and alteration of its carbon and nitrogen isotope composition during simulated and in situ early sedimentary diagenesis. Geochim. Cosmochim. Acta 66, 3573–3584.
Lessa, G.C., Angulo, R.J., 1998. Oscillations or not oscillations, that is the question—reply. Mar. Geol. 150, 189–196.
Malamud-Roam, F., Ingram, L.B., 2004. Late Holocene $\delta^{13}C$ and pollen records of paleosalinity from tidal marshes in the San Francisco Bay estuary, California. Quat. Res. 62, 134–145.
Martin, L., Bittencourt, A.C.S.P., Vilas Boas, G.S., 1982. Primeira ocorrência de corais pleistocênicos da costa brasileira: datação do máximo da penúltima transgressão. Ciênc. Terra 3, 16–17.
Martin, L., Suguio, K., Flexor, J.M., 1986. Shell middens as a source for additional information in Holocene shoreline and sea-level reconstruction: examples from the coast of Brazil. In: Van de Plasseche, O. (Ed.), Sea-Level Research: A Manual for the Collection and Evaluation of Data. Free University of Amsterdam, Amsterdam, pp. 503–521.
Martin, L., Dominguez, J.M.L., Bittencourt, A.C.S.P., 2003. Fluctuating Holocene sea levels in Eastern and Southeastern Brazil: evidence from multiple fossil and geometric indicators. J. Coast. Reas. 19, 101–124.
Martinelli, L.A., Victória, R.L., Matsui, E., Forsberg, B.R., Mozeto, A.A., 1988. Utilização das variações naturais de $\delta^{13}C$ no estudo de cadeias alimentares em ambientes aquáticos: princípios e perspectivas. Acta Limnol. Bras. 11, 859–882.
Megens, L., van der Plichta, J., Leeuwb, J.W., Smedes, F., 2002. Stable carbon and radiocarbon isotope compositions of particle size fractions to determine origins of sedimentary organic matter in an estuary. Org. Geochem. 33, 945–952.
Meyers, P.A., 1994. Preservation of elemental and isotopic source identification of sedimentary organic matter. Chem. Geol. 114, 289–302.
Meyers, P.A., 1997. Organic geochemical proxies of paleoceanographic, paleolimnologic, and paleoclimatic processes. Org. Geochem. 27, 213–250.
Meyers, P.A., 2003. Applications of organic geochemistry to paleolimnological reconstructions: a summary of examples from the Laurentian Great Lakes. Org. Geochem. 34, 261–289.
Middelburg, J.J., Nieuwenhuize, J., 1998. Carbon and nitrogen stable isotopes in suspended matter and sediments from the Schelde Estuary. Mar. Chem. 60, 217–225.
Milne, G.A., Long, A.J., Bassett, E., 2005. Modeling Holocene relative sea-level observations from the Caribbean and South America. Quat. Sci. Rev. 24, 1183–1202.
Miranda, A.C.C., Rossetti, D.F., 2009. Quaternary paleoenvironments and relative sea-level changes in Marajó Island (Northern Brazil): Facies, d13C, d15N and C/N. Palaeogeogr. Palaeoclimat. Palaeoecol. 282, 19–31.
Moraes-Neto, J.M., Alkimim, F.F., 2001. A deformação das coberturas terciárias do planalto da Borborema (PB-RN) e seu significado tectônico. Rev. Bras. Geociênc. 31, 95–106.
Mowbray, T., 1983. The genesis of lateral accretion deposits in recent intertidal mudflat channels, Solway Firth, Scotland. Sedimentology 30, 425–435.
Mulrennan, M.E., Woodroffe, C.D., 1998. Saltwater intrusion into the coastal plains of the Lower Mary River, Northern Territory. Austr. J. Environ. Manag. 54, 169–188.
Nakatsuka, T., Handa, N., Harada, N., Sugimoto, T., Imaizumi, S., 1997. Origin and decomposition of sinking particulate organic matter in the deep water column inferred from the vertical distributions of its $\delta^{15}N$, $\delta^{13}C$ and $\delta^{14}C$. Deep-Sea Res. 144, 1957–1979.
Nichols, M.M., Johnson, G.H., Peebles, P.C., 1991. Modern sediments and facies model for a microtidal coastal plain estuary, the James Estuary, Virginia. J. Sediment. Petrol. 61, 883–899.
O'Leary, M.H., 1988. Carbon isotopes in photosynthesis. Bioscience 38, 328–336.
Ogrinc, N., Fontolanb, G., Faganelic, J., Covellib, S., 2005. Carbon and nitrogen isotope compositions of organic matter in coastal marine sediments (the Gulf of Trieste, N Adriatic Sea): indicators of sources and preservation. Mar. Chem. 95, 163–181.
Pessenda, L.C.R., Gouveia, S.E.M., Aravenab, R., Bouletc, R., Valencia, E.P.E., 2004. Holocene fire and vegetation changes in southeastern Brazil as deduced from fossil charcoal and soil carbon isotopes. Quat. Int. 114, 35–43.
Peterson, B.J., Fry, B., Hullar, M., Saupe, S., Wright, R., 1994. The distribution and stable carbon isotope composition of dissolved organic carbon in estuaries. Estuaries 17, 111–121.
Plink-Bjorklund, P., 2005. Stacked fluvial and tide-dominated estuarine deposits in high frequency (fourth-order) sequences of the Eocene Central Basin, Spitsbergen. Sedimentology 52, 391–428.
Reinson, G.E., 1992. Transgressive barrier island and estuarine systems. In: Walker, R.G., James, N.P. (Eds.), Facies Models. Geol. Assoc. Can., Mem. Univ. Newfoundland, Newfoundland, pp. 179–194.
Ricketts, B.D., 1991. Lower Paleocene drowned valley and barred estuaries, Canadian Arctic Islands, aspects of their geomorphological and sedimentological evolution. In: Smith, D.G., Reinson, G.E., Zaitlin, B.A., Rahmani, R.A. (Eds.), Clastic Tidal Sedimentology. : Mem., 16. CSPG, Calgary, pp. 91–106.
Rossetti, D.F., 2000. Influence of low amplitude/high frequency relative sea-level changes in a wave-dominated estuary (Miocene), São Luís Basin, northern Brazil. Sed. Geol. 133, 295–324.
Rossetti, D.F., Valeriano, M.M., 2007. Evolution of the lowest Amazon basin modeled from the integration of geological and SRTM topographic data. Catena 70, 253–265.
Rossetti, D.F., Toledo, P.M., Góes, A.M., 2005. New geological framework for the Western Amazonia: implications for biogeography and evolution. Quat. Res. 63, 78–89.
Rossetti, D.F., Valeriano, M.M., Thales, M., 2007. An abandoned estuary within Marajó Island: implications for late Quaternary paleogeography of northern Brazil. Estuar. Coast. 30, 813–826.
Rossetti, D.F., Valeriano, M.M., Góes, A.M., Thalles, M., 2008a. Palaeodrainage on Marajó Island, northern Brazil, in relation to Holocene relative sea-level dynamics. Holoc. 18, 1–12.
Rossetti, D.F., Góes, A.M., Valeriano, M.M., Miranda, M.C., 2008b. Quaternary tectonics in a passive margin: Marajó Island, northern Brazil. J. Quat. Sci. 23, 121–135.
Sachs, J.P., Repeta, D.J., 1999. Oligotrophy and nitrogen fixation during eastern Mediterranean sapropel events. Science 286, 2485–2488.
Saino, T., Hattori, A., 1980. ^{15}N natural abundances in oceanic suspended particulate matter. Nature 283, 752–754.
Salomons, W., Mook, W.G., 1981. Field observations of the isotopic composition of particulate organic carbon in the southern North Sea and adjacent estuaries. Mar. Geol. 41, 11–20.
Sha, L.P., de Boer, P.L., 1991. Ebb-tidal delta deposits along the west Frisian Islands (The Netherlands): processes, facies architecture and preservation. In: Smith, D.G., Reinson, G.E., Zaitlin, B.A., Rahmani, R.A. (Eds.), Clastic Tidal Sedimentology. : Mem., 16. CSPG, Calgary, pp. 199–218.
Shackleton, N.J., 1988. Oxygen isotopes, ice volume, and sea level. Quat. Sci. Rev. 6, 183–190.
Sherr, E.B., 1982. Carbon isotope composition of organic seston and sediments in a Georgia salt marsh estuary. Geochim. Cosmochim. Acta 46, 1227–1232.
Shultz, D.J., Calder, J.A., 1976. Organic carbon $^{13}C/^{12}C$ variation in estuarine sediments. Geochim. Cosmochim. Acta 40, 381–385.
Souza-Filho, P.W.M., Paradella, W.R., 2003. Use of synthetic aperture radar for recognition of coastal geomorphological features, land-use assessment and shoreline changes in Bragança coast, Pará, northern Brazil. An. Acad. Bras. Ciênc. 75, 341–356.
Stirling, C.H., Esat, T.M., McCulloch, M.T., Lambeck, K., 1995. High-precision U-series dating of corals from Western Australia and implications for the timing and duration of the Last Interglacial. Earth Planet. Sci. Lett. 135, 115–130.
Szatmari, P., Fraçolin, J.B.L., Zanotto, O., Wolff, S., 1987. Evolução tectônica da margem equatorial brasileira. Rev. Bras. Geol. 17, 180–188.
Suguio, K., Martin, L., Bittencourt, A.C.S.P., Dominguez, J.M.L., Flexor, J.M., Azevedo, A.E. G., 1985. Flutuaçõees do nível relativo do mar durante o Quaternário superior ao longo do litoral brasileiro e suas implicações na sedimentação costeira. Revista Brasileira de Geociências 15, 273–286.
Talma, A.S., Vogel, J.C., 1993. A simplified approach to calibrating 14C dates. Radiocarbon 35, 317–322.
Terwindt, J.H.J., Breusers, N.H.C., 1972. Experiments on the origin of flaser, lenticular, and sand-clay alternating bedding. Sedimentology 19, 85–98.

Thornton, S.F., McManus, J., 1994. Applications of organic carbon and nitrogen stable isotope and C/N ratios as source indicators of organic matter provenance in estuarine systems: evidence from the Tay Estuary, Scotland. Estuar. Coast. Shelf Sci. 38, 219–233.

Toledo, M.B., Bush, M., 2008. A Holocene pollen record of savanna establishment in coastal Amapá. An. Acad. Bras. Ciênc. 80, 341–351.

Tomazelli, L.J., Dillenburg, S.R., 2007. Sedimentary facies and stratigraphy of a last interglacial coastal barrier in south Brazil. Mar. Geol. 244, 33–45.

Van der Hammen, T., Absy, M.L., 1994. Amazonia during Last Glacial. Palaeogeogr. Palaeoclimatol. Palaeoecol. 109, 247–261.

Van der Hammen, T., Duivenvoorden, J.F., Lips, J.M., Urrego, L.E., Espejo, N., 1992. The Late Quaternary of the middle Caquetá area (Colombian Amazonia). J. Quat. Sci. 7, 45–55.

Vedel, V., Behling, H., Cohen, M.C.L., Lara, R.J., 2006. Holocene mangrove dynsamics and sea-level changes in northern Brazil, inferences from the Taperebal core in northeastern Pará State. Veg. Hist. Archaeobot. 15, 115–123.

Wilson, G.P., Lamb, A.L., Leng, M.J., Gonzalez, S., Huddart, D., 2005a. $\delta^{13}C$ and C/N as potential coastal palaeoenvironmental indicators in the Mersey Estuary, UK. Quat. Sci. Rev. 24, 2015–2029.

Wilson, G.P., Lamb, A.L., Leng, M.J., Gonzalez, S., Huddart, D., 2005b. Variability of organic $\delta^{13}C$ and C/N in the Mersey Estuary, U.K. and its implications for sea-level reconstruction studies. Estuar. Coast. Shelf Sci. 64, 685–698.

Woodroffe, C.D., Chappell, J., Thom, B.G., Wallensky, E., 1989. Depositional model of a macrotidal estuary and floodplain, South Alligator River, Northern Australia. Sedimentology 36, 37–756.